# Inhibitory effects of SARS-CoV-2 nonstructural proteins on the RIG-I signaling pathway

MASTER'S THESIS

SUPERVISED BY:
MSc. RICKARD LUNDBERG
PROF. ILKKA JULKUNEN
INSTITUTE OF BIOMEDICINE
UNIVERSITY OF TURKU

University of Turku

Department of Biochemistry

Biochemistry

October 2021

Arttu Reinholm

*The originality of this thesis has been checked in accordance with the University of Turku quality assurance system using the Turnitin OriginalityCheck service.*

University of Turku

Department of Biochemistry

ARTTU REINHOLM: Inhibitory effects of SARS-CoV-2 nonstructural proteins on the RIG-I signaling pathway

Master's Thesis

58 pages

Biochemistry FM

10/2021

Severe acute respiratory syndrome coronavirus-2 (SARS-CoV-2) from the *Coronaviridae* family is an enveloped, spherical virus with a 30 kb long non-segmented positive single-stranded RNA genome, which encodes for 16 non-structural, four structural, and eleven accessory proteins. It was first discovered in 2019 in Wuhan, Hubei province, China, from a patient suffering from pneumonia caused by a previously unknown virus. SARS-CoV-2 rapidly spread throughout Wuhan, after which it spread around the world, leading to the current pandemic. The common symptoms caused by SARS-CoV-2 are fever, cough, dyspnea, and myalgia, similar to other human-infecting coronaviruses such as SARS-CoV and MERS-CoV, but less severe. SARS-CoV-2 has been shown to inhibit the RIG-I pathway, disrupting the production of type I and III interferons, and to evade host innate immune response.

In this study, I analyzed whether some SARS-CoV-2 proteins have an ability to inhibit the production of type III interferon by interfering with the RIG-I pathway. Additionally, I checked if the ORF9B accessory protein was immunogenic. To accomplish this, I cloned the genes of interest into mammalian expression vectors, which were then transfected to HEK-293 cells along with a constitutively active form of RIG-I and IFN-λ1 promoter luciferase reporter plasmid. Structural proteins were incapable of inhibiting RIG-I induced activation of type III interferon promoter, while nonstructural proteins Nsp1, Nsp6, and Nsp13 showed clear inhibitory activity. ORF9B was found not to be immunogenic.

Key words

RIG-I, SARS-CoV-2, nonstructural protein, luciferase, western blotting, interferon

# Table of contents

Abbreviations

1. Review of the literature....4
   - 1.1 Introduction....4
   - 1.2 Viruses....4
   - 1.3 Coronaviruses....6
   - 1.4 Clinical symptoms of COVID-19....9
   - 1.5 Epidemiology of SARS-CoV-2....10
   - 1.6 Innate immunity....11
   - 1.7 Adaptive immunity....12
   - 1.8 Interferons....12
   - 1.9 SARS-CoV-2 structure and genome organization....13
     - 1.9.1 Non-structural and accessory proteins....14
     - 1.9.2 Structural proteins....19
     - 1.9.3 Accessory proteins....21
   - 1.10 Replication cycle....22
   - 1.11 RIG-I pathway....23
     - 1.11.1 RIG-I....23
     - 1.11.2 MAVS....24
     - 1.11.3 Kinases associated with the RIG-I pathway....24
     - 1.11.4 Signaling pathway....25
2. Goal of the study....27
3. Materials and methods....28
   - 3.1 Plasmids....28
   - 3.2 Sera samples....28
   - 3.3 Cell lines....28
   - 3.4 Antibodies....28
   - 3.5 Cell culturing....29
   - 3.6 Western blotting....29
   - 3.7 Immunofluorescence assays (IFA)....30
     - 3.7.1 IFA using coverslips....30
     - 3.7.2 IFA in immunogenicity assays....31
   - 3.8 Luciferase assays....31
   - 3.9 Cloning....32
     - 3.9.1 Infusion cloning....32
     - 3.9.2 Restriction enzyme digestion and plasmid isolation....33
4. Results....35
   - 4.1 Expression of SARS-CoV-2 proteins....35
   - 4.2 SARS-CoV-2 structural proteins do not inhibit the RIG-I pathway....40
   - 4.3 SARS-CoV-2 Nsp1, Nsp6, and Nsp13 inhibit the activation of IFN-λ promoter....41
   - 4.4 SARS-CoV-2 ORF9B is not immunogenic....44
5. Discussion....47
6. Conclusions....51
7. Sources....53

## Abbreviations

| | | | |
|---|---|---|---|
| 2CARD | Tandem caspase activated recruitment domain | ICTV | International committee on taxonomy of viruses |
| ACE2 | Angiotensin converting enzyme 2 | IFA | Immunofluorescence assay |
| AGE | Agarose gel electrophoresis | IFN | Interferon |
| ARDS | Acute respiratory distress syndrome | IFNAR | Interferon-α-receptor |
| BSA | Bovine serum albumin | IKK-epsilon | Inhibitor of nuclear factor kappa-B kinase subunit epsilon |
| CFR | Case-fatality-ratio | IPS-1 | IFN-β-promoter stimulator 1 |
| COVID-19 | Coronavirus induced disease 19 | ISG | Interferon stimulated gene |
| CPE | Cytopathic effect | JAK-STAT | Janus kinase-signal transducer and activator of transcription |
| CTD | C-terminal domain | MAVS | Mitochondrial antiviral signaling protein |
| DAPI | 4',6-diamido-2-phynylindole | MERS | Middle East respiratory syndrome |
| DNA | Deoxyribonucleic acid | NSP | Non-structural protein |
| ER | Endoplasmic reticulum | PAGE | Polyacrylamide gel electrophoresis |
| ERGIC | Endoplasmic reticulum-Golgi intermediate compartment | PAMP | Pathogen associated molecular pattern |
| FADD | FAS-associated death domain | PCR | Polymerase chain reaction |
| FBS | Fetal bovine serum | PFA | Paraformaldehyde |
| GAPDH | Glyceraldehyde 3-phosphate dehydrogenase | PLpro | Papain-like protease |
| HA | Hemagglutinin | RdRp | RNA-dependent RNA-polymerase |
| HCV | Hepatitis C virus | RNP | Ribonucleoprotein |
| HEK-293 | Human embryonic kidney cells | $R_0$ | Basic reproduction number |
| HIS | Histidine | RSV | Rous sarcoma virus |
| HUH-7 | Human hepatocyte-derived carcinoma cells | SARS | Severe acute respiratory syndrome |

| | | | |
|---|---|---|---|
| SARS-CoV | Severe acute respiratory syndrome-corona virus | TRADD | Tumor necrosis factor receptor type 1-associated DEATH domain |
| SDS | Sodium dodecyl sulfate | RNA | Ribonucleic acid |
| TBK1 | TANK-binding kinase 1 | WB | Western blot |

## 1. Review of literature

### 1.1 Introduction

Severe acute respiratory syndrome coronavirus 2 (SARS-CoV-2) was first identified as the causative agent of coronavirus disease (COVID-19) in December 2019 and has since then spread to all continents except Antarctica, causing the ongoing pandemic that has by October, 2021 resulted in almost 240 million confirmed cases and over 5 million deaths (Johns Hopkins Coronavirus Resource Center). Like all other coronaviruses, it belongs to the *Coronaviridae*, a family of large, enveloped, positive-sense single-stranded ribonucleic acid (ssRNA) viruses that infect the upper respiratory tract. It is genetically closely related to severe acute respiratory syndrome coronavirus (SARS-CoV), which caused an epidemic in 2002.

Like the other coronaviruses, SARS-CoV has different mechanisms that it utilizes to evade or delay the host's immune response. These mechanisms have been studied extensively after the 2002 epidemic, and the sequence similarity of SARS-CoV with the SARS-CoV-2 may provide insight into its mechanisms as well. How SARS-CoV-2 evades the innate immune system, particularly the RIG-I pathway, is the topic of this study.

### 1.2 Viruses

Viruses are small particles that are reliant on other organisms to replicate their genome, produce necessary proteins for their function, and assemble the virion particles themselves. They are comprised of a usually small DNA or RNA genome, and a protective shell known as a capsid, which is comprised of repeating units of structural proteins known as capsomers, at minimum, although they often also have accessory proteins within the capsid, such as the tegument proteins within the capsid of herpes simplex virus 1. The capsid has receptor binding proteins on its surface, which make viruses entry into the host cell possible. Although animal viruses rely on receptors to gain access to the cells, plant viruses have no need for them. Instead, they infiltrate the cell in the aftermath of events that damage cell walls, and among various fluids that plants take from the soil and elsewhere. (Understanding Viruses 3rd Edition)

The most common shapes for viruses are icosahedral and helical, although other shapes such as brick-like or pleomorphic are also possible. The shape is determined by

the capsomers, of which there can be more than one type, that form the capsid. The capsid is the result of capsomers forming the lowest-energy conformation, which is the most stable form the capsid can take. The virus particle can either be naked or have one or more envelopes surrounding it. These envelopes are membranes taken from the host cells, and they provide an additional means of evasion against the immune defenses of the host. (Understanding Viruses 3rd Edition, Chapter 2)

The genome type varies between different virus species, and viruses can be classified into different groups according to the Baltimore system. According to this system, there are seven different virus types (Table 1). The genome type greatly influences the replication cycle of the virus, since negative-sense ssRNA and double-stranded deoxyribonucleic acid (dsDNA) virus genomes can be directly replicated by viral or cellular RNA polymerases. Positive sense RNA viruses need to produce their own polymerases and in the case of some types reverse transcriptase is also required. (Understanding Viruses 3rd Edition)

Due to the small genome size, virus proteins often perform multiple functions, maximizing the utility of their limited protein selection. (Understanding Viruses 3rd Edition)

*Table 1 Virus type classifications as according to the Baltimore system*

| Class | Genome type | Specifics |
|---|---|---|
| I | dsDNA | DNA-dependent RNA polymerase required |
| II | ssDNA | DNA-dependent DNA polymerase required |
| III | dsRNA | Viral RNA-dependent RNA polymerase required |
| IV | negative-sense ssRNA | Immediately transcribed by the host polymerase |
| V | negative-sense ssRNA | Viral RNA-dependent RNA polymerase required |
| VI | positive-sense ssRNA | Requires viral reverse transcriptase |
| VII | dsRNA | Requires viral reverse transcriptase |

### 1.3 Coronaviruses

Coronaviruses belong to the *Coronaviridae* family, the largest family in the order *Nidovirales* (ICTV). The name coronavirus comes from the distinct, sun-like silhouette formed by the capsid and the club-shaped receptors-binding proteins protruding from the surface, that are visible when observing the virions with electron microscopy. Earliest members of the *Coronaviridae* family were identified in the 1930s, but they were not grouped together until the 1960s. The coronaviruses that infect and cause respiratory symptoms in humans are part of the *Orthocoronavirinae* subfamily and are further divided into *alphacoronavirus* and *betacoronavirus* genera (Figure 1). In total, as many as 45 different coronavirus species have been discovered. These viruses collectively infect and cause disease to many different host species, which range from rodents to beluga whales. (ICTV) Out of these 45 viruses, 7 are pathogenic to humans (Table 2). The rates of coronavirus mutations are in the range of $10^{-4}$ mutations per year per site. This combined with the fact that different coronaviruses circulate in the same reservoirs and can recombine makes it likely that new strains capable of infecting and causing disease in humans will emerge. (Su et al. 2016; Wang et al. 2020)

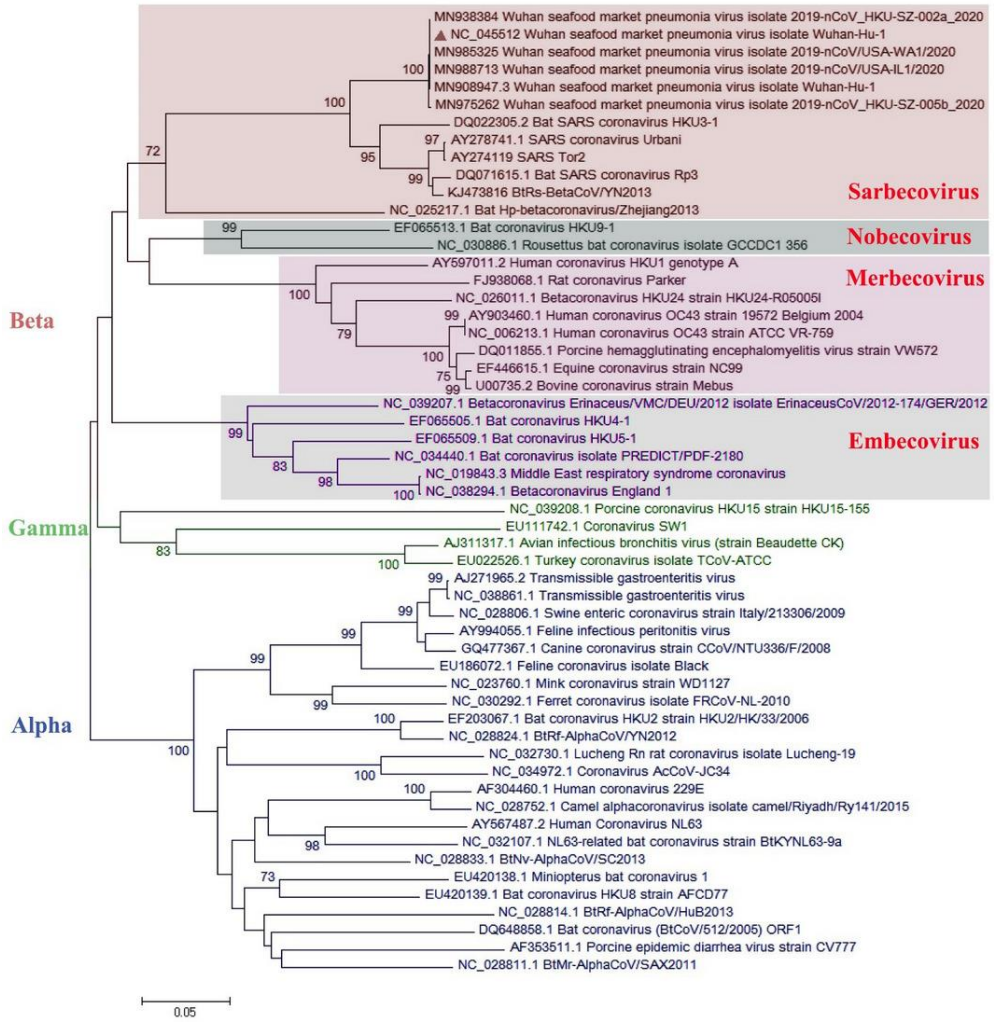


*Figure 1 Phylogenic tree of coronaviruses. (Tabibzadeh et al. 2021)*

*Table 1 List of human infecting coronaviruses that cause respiratory tract symptoms*

| Virus | Discovery year | Genus |
|---|---|---|
| HCoV-229E | 1966 | *alphacoronavirus* |
| HCoV-OC43 | 1967 | *betacoronavirus* |
| HCoV-NL63 | 2004 | *alphacoronavirus* |
| HCoV-HKU1 | 2005 | *betacoronavirus* |
| SARS-CoV | 2002 | *betacoronavirus* |
| MERS-CoV | 2012 | *betacoronavirus* |
| SARS-CoV-2 | 2019 | *betacoronavirus* |

HCoV-229E and HCoV-OC43 were the first human-infecting coronaviruses to be discovered, in 1966 and 1967 respectively (Hamre and Procknow 1966; McIntosh et al. 1967). HCoV-229E sequence does not vary much between isolates from different regions, whereas HCoV-OC43 sequence does, even in the same region (Fields Virology 6th Edition, Chapter 28, p. 844). While HCoV-229E utilizes the ANPEP receptor when entering to the cell, HCoV-OC43 uses a different receptor that remains to be identified (Forni et al. 2016). These viruses were isolated from patients suffering from upper respiratory symptoms in the late 1960s. Both of these viruses are seasonal, circulating the populace and causing outbreaks around the globe during winter and early spring. They are responsible for 15-29% of all respiratory tract infections, causing mild flu-like symptoms. (Su et al. 2016)

SARS-CoV was first isolated in 2002 in the Guangdong province, People's Republic of China. SARS-CoV enter the cell by binding to the ACE2 receptor. Although civets were first suspected to be the main reservoir for the virus, horseshoe bats were later indicated as the primary reservoir, due to a large amount of bat coronavirus strains that were very similar to SARS-CoV. (Cui et al. 2019) What made it notable was its ability to cause severe, in some cases fatal, illness in individuals with no underlying problems with health, with a case-fatality -ratio (CFR) of 11% (Chang-Yeung and Xu 2003). This sparked considerable interest in coronaviruses and led to the development of new viral RNA detection assays, utilizing PCR, that were very coronavirus species specific. Currently, SARS-CoV is not circulating in the human population (https://www.cdc.gov/sars/index.html).

The new sensitive viral RNA detection assays led to the discovery of new coronavirus species that are mildly pathogenic to humans, NL63 and HKU1. When a nasal swab taken in 1982 from an 8-month-old boy suffering from pneumonia caused by an unknown pathogen was tested with one of these new RNA detection assays, NL63 was discovered. NL63 uses ACE2 to enter the host cell. A year later, another coronavirus species known as HKU1 was isolated from a 71-year-old patient in Hongkong, once again by being detected with a SARS-CoV-specific PCR assay. Both of these newly discovered coronaviruses circulate the world seasonally. (Fouchier et al. 2004; Vabret *et al.* 2005)

In 2012, a new deadlier species, MERS-COV, was isolated from a 60-year-old man in Jeddah, Saudi Arabia (Zaki *et al.* 2012). Unlike other coronaviruses, MERS-CoV infections could lead to serious complications by causing renal failure, in addition to causing acute respiratory distress syndrome (ARDS). MERS-CoV attaches to the CD26 receptor on the surface of the host cell, similarly to HKU4, which is a bat coronavirus, and evolutionary most closely related to MERS-CoV (Lu et al. 2013). With a CFR of 36%, MERS-CoV is the most severe coronavirus species to humans (WHO). Currently, MERS-CoV is not circulating in the human population.

SARS-CoV-2 was first identified in Wuhan, Hubei province, in the People's Republic of China. It was isolated from several patients with upper-respiratory-system-related symptoms. (Zhu *et al*. 2020) Of the early cases, 66% of the patients were exposed in the Wuhan seafood market area (Huang et al. 2020). Like SARS-CoV, it can cause severe complications via ARDS and uses ACE2 as a primary receptor to enter the host cell (Arya et al. 2021). With a CFR of ca. 2%, it is less lethal than SARS-CoV and MERS-CoV, but it spreads more efficiently due to its high basic reproduction number (R0) of 3 (Wang et al. 2020). The evolutionary origin of SARS-CoV-2 is still under debate and several theories for the possible origin have been suggested. Many of these theories propose a spillover event from one of the many animal species sold in the Wuhan seafood market. For example, many proteins of the bat coronavirus RaTG13 have highly similar sequences compared to their counterparts in SARS-CoV-2. Some, like E and Nsp7 have an identical sequence, while others are very close, like RdRp with 96,2% sequence similarity with the corresponding SARS-CoV genes. Other possible reservoir animals include minks and pangolins. (Wang et al. 2020; Andersen et al. 2020)

### 1.4 Clinical symptoms of COVID-19

Symptoms of SARS-CoV-2 infection resemble those of the influenza viruses: Dyspnea, fever, coughing, and myalgia are present in many cases. Rarer symptoms include headache, confusion, and a sore throat. (Figure 2.) In severe cases, SARS-CoV-2 infection may result in ARDS, a potentially fatal condition. Patients with dyspnea and low oxygen concentration in blood are at a greater risk of developing ARDS rapidly (Tu et al. 2020). Asymptomatic individuals make up a significant portion of all cases, although estimates of exact percentage vary (Oran and Topol 2020).

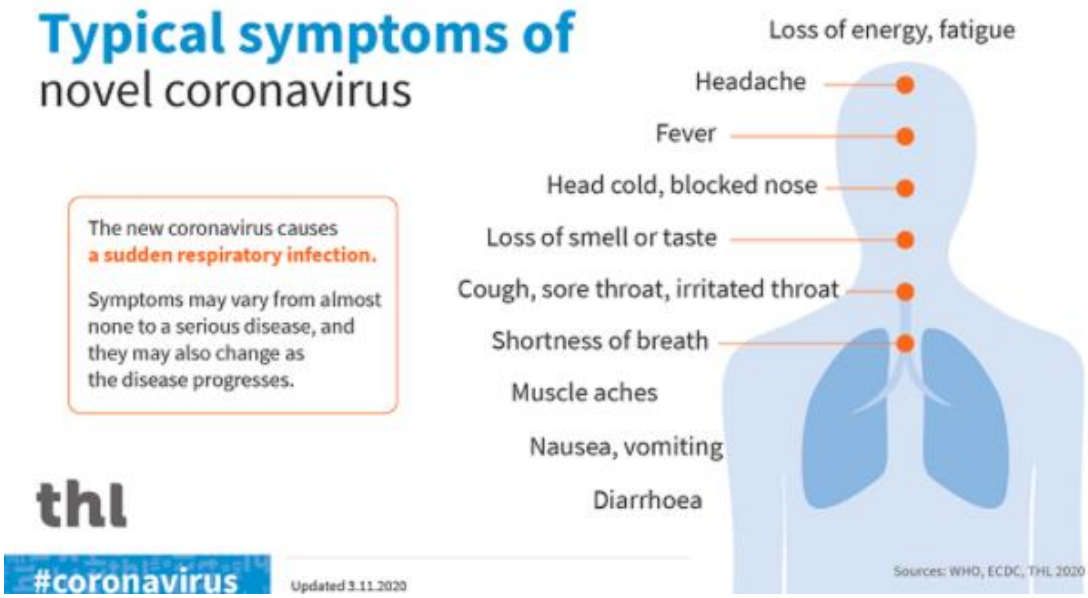


*Figure 2 Typical symptoms caused by SARS-CoV-2 (Finnish Institute for Health and Welfare)*

### 1.5 Epidemiology of SARS-CoV-2

As of 5th October, 2021, SARS-CoV-2 has a mortality rate of ca. 2%, not accounting for unconfirmed cases due to lack of testing, and has caused a total of 238 million infections (Johns Hopkins Coronavirus Resource Center). Most of the deaths are among elderly patients, 60 years old and up, with the likelihood of fatal complications increasing with age. Other factors, such as the quality of health care provided, also affect the fatality rates. (Tu et al. 2020) The spread of SARS-CoV-2 was rapid: After the first reported death in People's Republic of China on 9th January 2020, the first death out of People's Republic of China was reported on 1st February 2020, and the first death out of Asia on 14th February 2020. A month later, the virus had spread and caused fatalities worldwide in every continent except Antarctica. (Kumar et al. 2020) By comparison, Spanish flu took around 4 months to spread to every continent, barring Antarctica (Spinney 2018).

After the initial spread of the Wuhan variant, several mutant strains of SARS-CoV-2 have emerged. Most notable of these are the British variant B.1.1.7, the South African variant B.1.351, the Brazilian variant P.1, and the Indian variant B.1.617.2, also known as alpha, beta, gamma, and delta variants, respectively (https://www.who.int/en/activities/tracking-SARS-CoV-2-variants/). These four

variants belong to the variants of concern in many countries, since they have mutations that make them more likely to spread from human to human and provide enhanced resistance against vaccines that are designed based on the original strain. (Chakraborty et al. 2021)

### 1.6 Innate immunity

Immunity is divided into two parts: innate and adaptive immunity. Innate immunity is a collection of mechanisms that protect the organism from pathogens. These mechanisms are the first responders to pathogen invasions, enacting defenses against pathogens within minutes to hours after their entry into the host. Compared to the adaptive immunity, innate immunity is much less specific, allowing it to interact with multiple different pathogens immediately after encountering them. Adaptive immunity is much more specific and efficient but takes days to weeks to develop after the primary infection starts. However, if the same pathogen infects the host later, adaptive immune responses to this secondary infection take place much faster. (Kuby Immunology 7$^{th}$ edition, Chapter 5)

Mechanical barriers, like skin, are the first defenses against pathogens. As well as being physical barriers, surfaces also secrete antimicrobial proteins, such as lactoferrin, that inhibit the growth of bacteria or destroy them (Bulet et al. 2004). If these barriers are damaged and breached, such as by insect bites or mechanical stress, or the pathogens bypass them by different means, other innate immunity mechanisms join the fray.

Phagocytic cells, such as macrophages, often are the first cells to respond to any pathogens that have found their way into the host. They engulf the pathogens and destroy them with chemical cocktails that contain damaging compounds, like reactive oxygen species. The engulfment may take place without any assisting proteins, or the pathogens may be first opsonized to enhance phagocytosis. (Aderem and Underhill 1999)

The complement system is another powerful mechanism associated with innate immunity. It consists of several different proteins located in the serum that cleave each other, resulting in different cascades that have various effects on the invading pathogens. These cascades are initiated by three different pathways: the classical, the

alternative, and the lectin pathway. All of the pathways produce C3 convertases, which play an integral role in different mechanisms that include opsonization of bacteria, formation of membrane attack complexes, and interactions with the adaptive branch of immunity, to name a few. (Dunkelberger and Song 2010)

In addition to previous mechanisms, cells have a plethora of receptors on inside and on their surface, which trigger various different inflammatory, antiviral, and other signaling pathways upon binding to specific ligands. This is done with various pattern recognizing receptors (PRRs), which detect and bind to common secondary structures or post-translational modifications present in pathogens, called pathogen associated molecular patterns (PAMPs) (Unterholzner and Bowie 2008).

### 1.7 Adaptive immunity

Adaptive immunity is the part of the immune system which is acquired through exposure to viruses, bacteria, and other pathogens. When the adaptive immune system encounters a new pathogen, T lymphocytes are activated, leading to the development of cell-mediated immunity. B lymphocytes are also activated, producing antibodies against the invading pathogens. Some of the generated B lymphocytes will be memory cells, giving the organism the ability to remember antigens that have invaded it. This immunological memory is the backbone of adaptive immunity, allowing the organism to respond to secondary infections fast and specifically. (Palm and Medzhitov 2009; Sun et.al 2011)

### 1.8 Interferons

Interferons (IFNs) are a family of cytokines, which were discovered in the late 1950s (Isaacs and Lindenmann 2015). Interferons are divided in to three groups, type I, II, and III, which have various effects on both innate and adaptive immunity. As part of the innate immune system, interferons are among the first proteins that prime the cells to an antiviral state (Sadler and Williams 2008).

Type I interferons are 18-20 kDa large proteins with a helical structure that are divided into two major subgroups, interferon-α and interferon-β, and several minor subgroups (Kuby Immunology 7$^{th}$ edition, Chapter 5; Sadler and Williams 2008). Both major subgroups are secreted by activated macrophages and dendritic cells, as well as by

cells infected with viruses. (Samuel 2001; Zdrenghea et al. 2015) Once secreted, interferons interact with membrane-bound receptors such as type I IFN receptor (IFNAR) 1 / 2 heterodimer, activating JAK-STAT signaling pathways that culminate in the production of interferon-stimulated genes (ISGs) (Sadler and Williams 2008). These ISGs trigger the production of a variety of different proteins, such as ribonucleases, which destroy both host and virus RNA. Destruction of the host cells' RNA also inevitably leads to the death of the host cell itself, preventing the spread of viral infection to other cells. (Samuel 2001) ISGs also enhance host's virus -resistance in a myriad of other ways, like by upregulating RIG-I expression (Sadler and Williams 2008).

Type II interferon, also known as interferon-γ, influences the adaptive immunity by directing the T- helper cells to form more $T_H1$ type cells, and by activating multiple immune cell types. Type II interferon also induces antiviral responses especially against DNA viruses. Type II interferon structure differs greatly from type I interferons and it binds to a different receptor, interferon gamma receptor (IFNGR). (Samuel 2001; Schroder et al. 2004)

Type III interferons, or interferon-λ, are the most recent group of interferons, discovered in 2003. Their effects are similar to the type I interferons. Their structure is closely related to IL-10 family cytokines. Type III interferons bind to class II chemokine receptor (IFN- λR). Unlike IFNAR, which is expressed by all nucleated cells, IFN-λR is only expressed by epithelial cells, such as in the gut. (Gad et al. 2009; Wack et al. 2015)

### 1.9 Sars-CoV-2 structure and genome organization

SARS-CoV-2 enters the cell by binding to angiotensin-converting enzyme 2 (ACE2) and co-receptor transmembrane protease serine 2 (TMPRSS22), after which the viral and host membranes fuse, releasing the helical nucleocapsid to the cytoplasm (Kumar et al. 2020; V'kovski et al. 2020). Neuropilin-1 (NRP-1) has also been shown to aid SARS-CoV-2 to enter host cells and enhance infection in Hek-293T cells (Cantuti-Castelvetri et al. 2020).

SARS-CoV-2 RNA genome is approximately 30 kb long, and it has 14 open reading frames (ORF), which encode for 4 structural proteins, 16 non-structural proteins (Nsp), and 11 accessory proteins (Arya et al. 2021). The non-structural proteins are translated

from the two largest ORFs, ORF1a and ORF1b, as polyprotein precursors pp1a and large pp1ab. Pp1ab is translated when a -1-ribosome frameshift bypasses the stop codon of ORF1a, allowing the translation to continue through ORF1b. Polyproteins are cleaved to individual proteins by viral proteases such as Nsp3, which has a papain-like-protease domain, while the structural and accessory proteins are translated as individual proteins from the smaller ORFs. (Chen et al. 2020; Chan et al. 2020) The genome is flanked by untranslated regions (UTR), which have secondary structures that are important in the replication cycle (Huston et al. 2021). The 5'-end is capped with a 5'-methylguanosine cap and the 3'-end contains a Poly(A) tail, mimicking the structure of host mRNA and allowing viral mRNA to be translated by the host translation machinery (Chen et al. 2020; Huston et al. 2021).

### 1.9.1 Non-structural proteins

Non-structural proteins are proteins responsible for the replication process of the virus. They accomplish this by hijacking the protein production machinery of the host cell, as well as by producing viral complexes essential to the replication cycle or survival of the virus. Characteristically to virus proteins, coronavirus Nsps often have multiple roles, such as an inhibitor of one of the many innate immunity responses. (Figure 3, Table 3) The close sequence similarity of the SARS-CoV-2 genome to the more studied coronaviruses makes it possible to deduce the likely functions of the SARS-CoV-2 proteins.

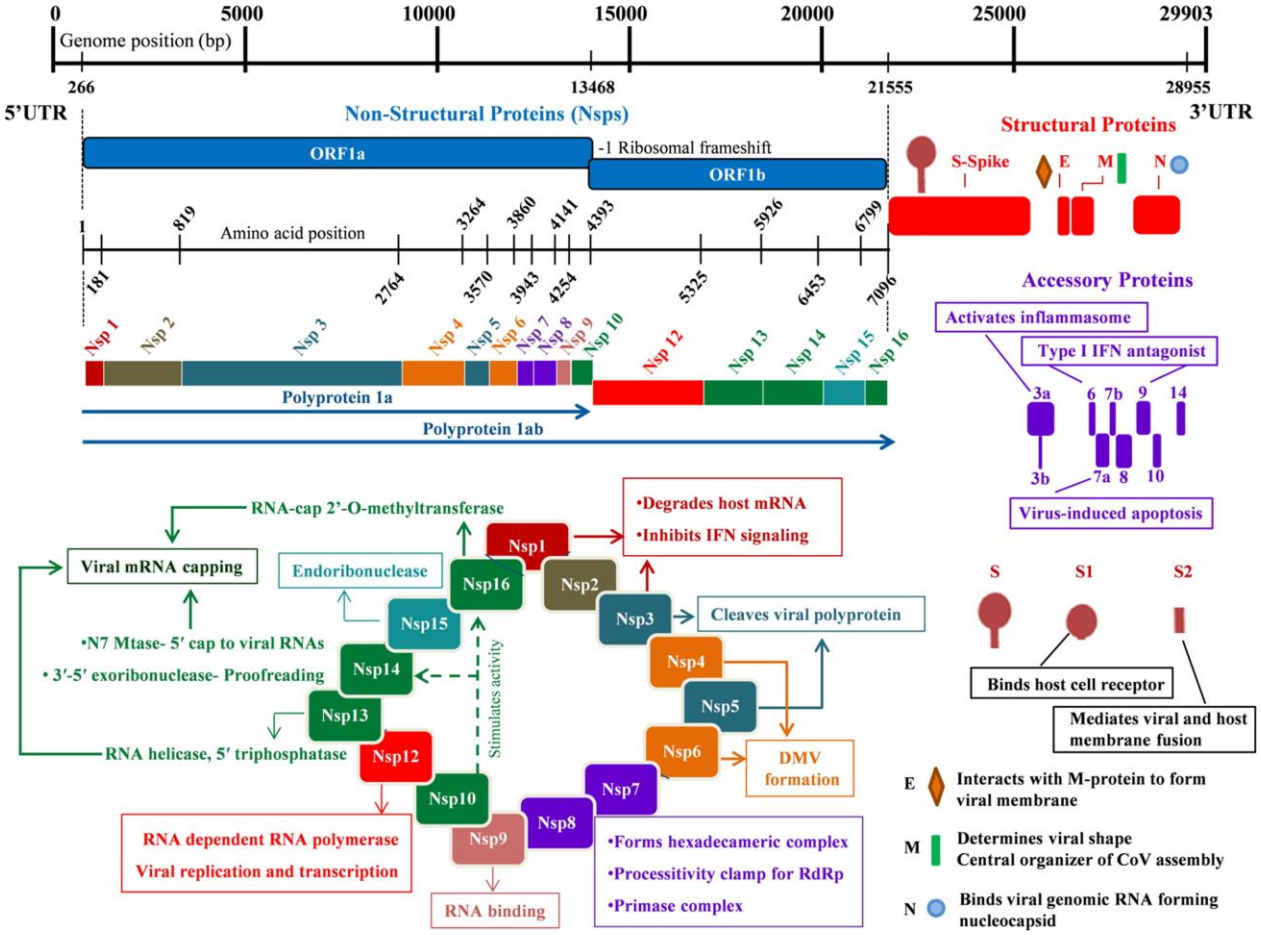


*Figure 3 SARS-CoV-2 proteins encoded from the genome and cleaved from the primary amino acid chain, with proposed functions. (Arya et al. 2021)*

*Table 2 Non-structural and structural proteins of SARS-CoV-2 and their primary functions*

| Protein | Function |
|---|---|
| Nsp1 | Inhibits host cells protein synthesis |
| Nsp2 | Not known |
| Nsp3 | Scaffolding, cleaves viral polyproteins |
| Nsp4 | Membrane restructuring |
| Nsp5 | Protease |
| Nsp6 | Inhibits type I interferon response |
| Nsp7 | RNA primase |
| Nsp8 | Part of the primase complex |
| Nsp9 | Phosphatase |
| Nsp10 | Scaffolding protein |
| Nsp11 | Not known |
| Nsp12 | Catalytic subunit of RdRp |
| Nsp13 | Helicase |
| Nsp14 | Proofreading and methylation of mRNA |
| Nsp15 | Cleaves RNA |
| Nsp16 | 2-O-methyltransferase |
| Spike | Receptor binding |
| Envelope | Participates in viral membrane formation |
| Membrane | Organizes virion assembly |
| Nucleocapsid | Protects the genome |

Nsp1 is a 19,8 kDa protein that inhibits host cell protein synthesis by binding to the 40S ribosomal subunit, blocking the mRNA entry channel with its C-terminal domain, and by degrading host mRNA (Gordon et al. 2020; Schubert et al. 2020). Its production is initiated in the early stage of infection by it being cleaved from the N-terminus of polyprotein precursors pp1a and pp1ab by papain-like protease (PLpro) (Arya et al. 2021). SARS-CoV Nsp1 has been implicated in the suppression of the host's innate immunity by inhibiting type I interferon expression, although the mechanisms for this are not fully known. Since there is considerable amino acid sequence similarity (84%)

between SARS-CoV-2 and SARS-CoV Nsp1 proteins, it is possible that SARS-CoV-2 Nsp1 has a similar inhibitory function. (Lei et al. 2020; Xia et al. 2020; Suruyawanshi et al. 2021)

Nsp2 is 638 amino acids long, 70,5 kDa protein which function is still unknown. It has also been shown to interact with strumpellin, which regulates actin assembly in intracellular vesicles and may help the virion particles to exit the cell after maturation. (Seaman et al. 2013; Gordon et al. 2020; Ma et al. 2021) In SARS-CoV, Nsp2 also disturbs the host's intracellular signaling by interacting with prohibit 1 and 2, modulating the cell survival signaling pathway (Cornillez-Ty et al. 2009). Because its sequence similarity with SARS-CoV Nsp2 is only 76,8%, the functions may be different (Ma et al. 2021).

Nsp3 is 1945 amino acids long, 217,3 kDa protein, which makes it the largest protein encoded by SARS-CoV-2 (Gordon et al. 2020). Nsp3 is a multidomain, membrane bound protein with multiple functions, such as acting as scaffolding for viral and host proteins. It has also been shown to delay the activation of IFN-β (Lei et al. 2020). In SARS-CoV Nsp3, the PLpro domain not only cleaves polyprotein precursors, but also inhibits type I interferon signaling by interfering with STING-TRAF3-TBK1 complex (Harcourt et al. 2004; Chen et al. 2014). Macrodomain X is a conserved domain in coronaviruses, and it inhibits type I interferon response by interfering with ADP-ribosylation (Claverie 2020). (Lei et al. 2018)

Nsp4 is 56,2 kDa protein and has not been well studied in SARS-CoV-2, but since it has a fairly high sequence similarity (80%) with its SARS-CoV counterpart, it may similarly contribute to viral replication by rearranging membranes to create viral protein factories. (Gordon et al. 2020; Arya et al. 2021; Suruyawanshi et al. 2021)

Nsp5 is a 33 kDa protease that cleaves pp1a and pp1ab with the 3CL-pro domain to create 12 different proteins (Gordon et al. 2020). It also regulates gene expression and inhibits innate immune response by reducing nuclear translocation of HDAC2, an important epigenetic modifier, and by cleaving TAB1. (Suruyawanshi et al. 2021; Moustaqil et al. 2021)

Nsp6 is a 33 kDa protein and has been shown to inhibit type I interferon response by interacting with TBK1, leading to the inhibition of IRF3 phosphorylation. SARS-CoV Nsp6 restricts the size of hosts autophagosomes, reducing the degradation rate of viral cytoplasmic proteins, while also generating autophagosomes for the viral proteins to exploit. (Cottam et al. 2014; Gordon et al. 2020; Xia et al. 2020)

Nsp7 is a 9,2 kDa conserved protein in SARS-CoV-2 and SARS-CoV, which forms an RNA primase complex with Nsp8, which in turn is part of the replicase complex (Te Velthuis, Aartjan J. W et al. 2012; Gordon et al. 2020). SARS-CoV-2 Nsp7 may also downregulate Rho GTPase expression and influence the organization of the host cell cytoskeleton, as well as inhibit IFN-α signaling (Bouhaddou et al. 2020; Xia et al. 2020).

Nsp8 is a 22 kDa protein which is another conserved protein in SARS-CoV-2 and SARS-CoV that participates in the formation of replication complex by being part of the primase complex (Te Velthuis, Aartjan J. W et al. 2012; Gordon et al. 2020). It has not been shown to interfere with the RIG-I pathway or interferon production (Lei et al. 2020).

Nsp9 is 12,4 kDa phosphatase that binds ssRNA as part of the replication-transcription complex (Egloff et al. 2004; Gordon et al. 2020). It has also been shown to increase virulence of the virus, be involved in viral RNA processing, and to have a stimulatory effect on type I IFN response (Egloff et al. 2004; Lei et al. 2020). SARS-CoV-2 Nsp9 has 97% sequence similarity with its SARS-CoV counterpart, which makes it highly probable that it also must form a dimer to function properly (Littler et al. 2020).

Nsp10 is a 14,8 kDa accessory protein that acts as scaffolding to Nsp14 and Nsp16, which has very high sequence similarity with its SARS-CoV counterpart (Gordon et al. 2020). SARS-CoV Nsp10 forms a complex with Nsp16 that assists with the processing of viral mRNA by methylating its 5'guanosine cap, making it harder for RIG-I to detect the viral mRNA. In the case of Nsp14, Nsp10 activates its proofreading and RNA editing capabilities. (Bouvet et al. 2014)

Nsp11 is a 1,3 kDa byproduct from the cleavage of pp1a (Gordon et al. 2020). Its function is still unknown (Arya et al. 2021).

Nsp12 is a 103 kDa catalytic subunit of the SARS-CoV-2 RNA-dependent RNA polymerase (RdRp) (Gordon et al. 2020). Its 554 amino acids long C-terminal RdRp domain contains a catalytical site, which enables Nsp12 to replicate the viral genome. To fully function, it must form a replicase complex with Nsp7 and Nsp8. (Hillen et al. 2020; Gao ja muut 2020) Nsp12 has been shown to inhibit IFN-β expression (Lei et al. 2020).

Nsp13 is a 67 kDa helicase, which is another protein that participates in the replicase-complex (Gordon et al. 2020). SARS-CoV Nsp13 unwinds RNA/DNA duplexes and is involved in 5'-RNA capping (Tanner et al. 2003). Its sequence identity with its SARS-CoV counterpart is nearly 100%, differing only by one amino acid, suggesting that the functions are similar (Chen et al. 2020). Nsp13 has been shown to inhibit IFN-β signaling in a similar fashion as Nsp6, as well as inhibiting IFN-α signaling (Xia et al. 2020).

Nsp14 is a 60 kDa protein with two distinct functions. Its N-terminal exonuclease domain proofreads viral mRNA, removing incorrect nucleotides. (Gordon et al. 2020) The C-terminal guanine-N7 methyl transferase methylates 5-capped mRNA, allowing viral mRNA to avoid detection by host PRRs (Bouvet et al. 2014). Nsp14 interferes with the IFN-β pathway by inhibiting IRF3 from reaching the nucleus (Lei et al. 2020).

Nsp15 is a 36,9 kDa conserved, negative-sense RNA cleaving, uridylate-specific endoribonuclease, which has also been implicated in blocking IRF3 localization to the nucleus. (Gordon et al. 2020; Arya et al. 2021)

Nsp16 is a 33,3 kDa 2-O-methyltransferase, which like Nsp14 methylates the 5-cap of viral mRNA to help the virus to avoid the host PRRs. It interferes with the IFN response when complexed with Nsp10. (Bouvet et al. 2014; Gordon et al. 2020)

### 1.9.2 Structural proteins

Structural proteins form the virion particle and protect the genome that is encased within the capsid. Besides providing the genome protection from the harsh environment outside and inside the cell, structural proteins have other equally important tasks, such as binding to the receptors of the host cell, assisting in the self-assembly of the virion or stabilizing the genome. Structural proteins are most likely

immunogenic, since they are exposed to the various innate immunity receptors and cells within the host. (Understanding Viruses 3rd edition, Chapter 2)

Spike (S) protein is a 1273-amino-acids long, 141,2 kDa, homo-trimeric, and club-shaped structural protein that is essential for receptor-mediated entry into the host cell. It has two subunits, S1 and S2. Two distinct domains, the receptor-binding domain facilitating the virus's attachment to the ACE2 receptors, and an N-terminal galectin-like domain are located in the S1 subunit (Arya et al. 2021). The function of the N-terminal galectin-like domain is not entirely clear, but it may stabilize the S2 domain in its prefusion conformation (Walls et al. 2020). Fusion of the host cell and virus membranes is mediated by the S2 subunit, which has four distinct structural motifs: fusion peptide, heptad repeats 1 and 2, and a transmembrane region (Wrapp et al. 2020). The S2 subunit has two different conformations, prefusion and postfusion. Transition from prefusion to postfusion is initiated by the host proteases after the receptor-binding domain (RBD) in S1 binds to the ACE2, altering the trimer conformation and exposing a cleavage site on the S2 subdomain (Renhong et al. 2020). The cleaving events are enhanced by co-receptor TMPRSS22. A separate furin cleavage site unique to SARS-CoV-2 is located between these subunits, the cleavage of which enhances the penetration of the virus into the host cell (Walls et al. 2020). S protein has not been shown to interfere with interferon responses. S protein mutations play a central role in different variants, since they can alter the receptor specificity of SARS-CoV-2 (Chakraborty et al. 2021).

Envelope (E) protein is a 75-amino-acids long, 8-12 kDa transmembrane protein that is part of the virion's envelope. Although it is expressed in only limited amounts, it is critical for the infectivity of the virus, as seen by the virus's failure to propagate in mutant strains that lack E protein. It has three different domains: an N-terminal hydrophilic domain, a single-helix transmembrane domain, and a hydrophilic C-terminal domain. E protein has not been shown to inhibit interferon response, instead it has a stimulatory effect on the ISGs. (Sarkar and Saha 2020; Arya et al. 2021; Suruyawanshi et al. 2021)

Membrane (M) protein is a 222-amino-acids long, 25-30 kDa transmembrane protein with three distinct domains: an N-terminal domain outside of the envelope, a triple-

helix transmembrane domain, and a C-terminal domain inside the virion. Like the E protein, it participates in the formation of the envelope, where most of its structure is buried (Gordon et al. 2020; Thomas 2020). From the four structural proteins, it's expressed the most. M protein has been shown to inhibit the activation of interferon-β (Lei et al. 2020).

Nucleocapsid (N) protein is 422 amino acids long, 43-50 kDa protein with two major domains, N-terminal and C-terminal, and is located inside the virion. Both domains are globular, contain several disordered regions, and are linked by a linker region, which is also disordered (Schiavina et al. 2021). The N-terminal domain's primary function is to bind to RNA, while the C-terminal domain regulates the formation of N homodimers. Both also have other functions. Several monomers of N cover the viral RNA, forming a ribonucleoprotein complex (RNP) with M proteins, stabilizing the viral genome, and shielding it from damage. The N protein interacts with the rest of the structural proteins when virions are being assembled to envelope the RNA and it has not been shown to inhibit interferon production. (Ye et al. 2020; Arya et al. 2021; Suruyawanshi et al. 2021)

### 1.9.3 Accessory proteins

SARS-CoV-2 has 11 accessory proteins which have distinct functions, some of which are unknown, and while they are not essential for the replication of the virus, they enhance the pathogenicity of SARS-CoV-2. The accessory proteins are involved in the suppression of the host cell antiviral response, and some of them directly interfere with type-I interferon pathways. All of the accessory proteins are small in size, with ORF3B being the largest at 227 amino acids. Some of the accessory proteins have undergone through mutations in the more pathogenic SARS-CoV-2 variants and may thus contribute to the pathogenicity of these variants. (Redondo et al. 2021).

### 1.10 Replication cycle

Replication cycles of viruses are an important field of study (Figure 4.). By identifying proteins or protein complexes that are essential for the replication of the virus and do not interfere with the normal functions of the host cell too severely, it is possible to target these proteins with antiviral drugs, halting the replication cycle of the virus and thus hamper the spread of the infection. Prime targets for these antiviral drugs are the viral proteins that are essential for the replication cycle, such as viral RdRp since the host cell has no need for them and is not harmed by their absence.

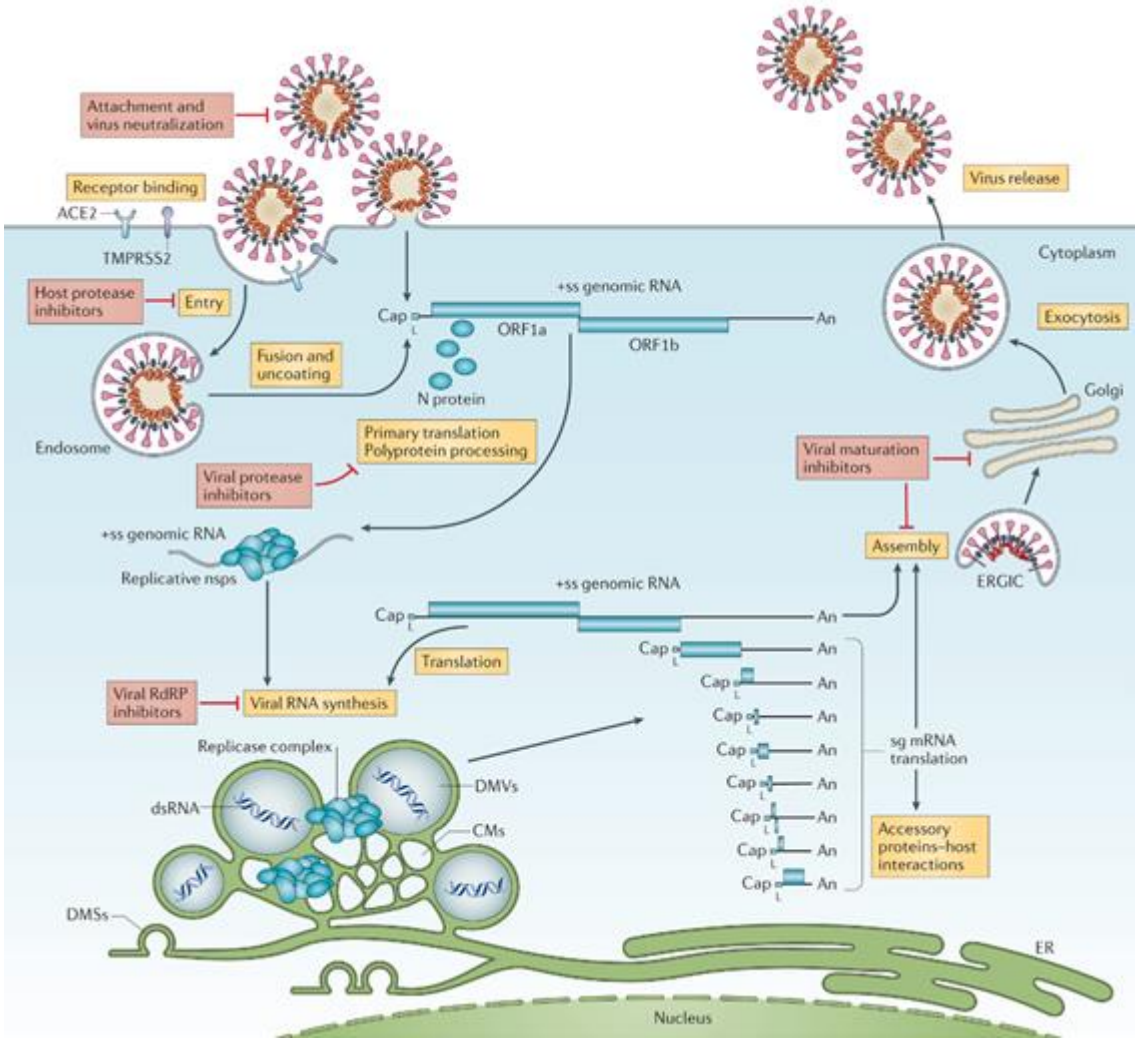


*Figure 4 Different stages of the SARS-CoV-2 replication cycle (V'kovski et al. 2020, modified)*

After accessing the host's respiratory tract, the virion attaches to the epithelial cell by binding to its primary receptor ACE2 on the surface of the cell membrane. Secondary receptor TMPRSS2 primes the S protein for binding by cleaving it. Binding triggers conformational changes in the S protein on the surface of the virion and leads to the fusion of the virion's envelope and host cells membrane, releasing the viral RNA into the cytosol of the host cell. Proteases present in the cell and environmental factors, such as pH, also play a role in the fusion event. (Hoffmann et al. 2020)

After the coated viral RNA is released to the cytoplasm, it starts to be degenerated by host cells proteases, leading to the uncoating of the viral RNA. This RNA is immediately translated in to two polyprotein precursors, which are autocleaved and processed further by the autocleavage products. Some of the cleaved proteins are post-translationally modified in the endoplasmic reticulum (ER), for example by glycosylation. The RNA is also used as a template for genomic and subgenomic negative-sense ssRNA. The former is used to form new virions and the latter as a template for positive-sense ssRNA, which are translated into more viral proteins. (V'kovski et al. 2020)

The virus particles are assembled in the ER, endoplasmic reticulum-Golgi intermediate compartment (ERGIC), and the Golgi apparatus itself, where most of the particle assembly happens (Astuti and Ysrafil 2020). The newly synthesized viral genomic RNA interacts with the structural proteins that are translocated into the Golgi, and new virions are formed. Fully assembled particles are secreted via exocytosis. (Chen et al. 2020)

### 1.11 RIG-I pathway

Retinoic acid-inducible-gene-I (RIG-I) pathway is one of the innate immunity mechanisms that is activated when virus RNA is detected by the RIG-I receptor. This pathway triggers the production of different types of interferons, which in turn activate a JAK-STAT pathway, culminating in the expression of interferon-stimulated genes, which encode antiviral proteins such as dsRNA-activated protein kinase, also known as PKR. (Sadler and Williams 2008; Onomoto et al. 2021).

### 1.11.1 RIG-I

RIG-I is a soluble PRR, which is present in the cytosol of most cell types. It differentiates between viral RNA and host RNA by recognizing structural differences, pathogen-associated molecular patterns (PAMP). Such PAMPs include double-stranded regions of the RNA, polyuridine sequences, and 5' triphosphate modification that is done to the viral RNA when it is processed, or which is already present in some viruses. RIG-I has two RNA binding domains, DECH helicase and C-terminal domain (CTD). Its tandem caspase activation recruitment domain (2CARD) is blocked by the helicase domain when viral RNA is not bound to prevent unintended activation which might lead to a cytokine storm, damaging the host. Upon RNA binding to the CTD-domain, the conformational change exposes the 2CARD, allowing it to oligomerize and form a tetramer, which in turn is capable to interact with the next signaling component. (Loo and Gale 2011; Schlee 2013; Onomoto et al 2021)

### 1.11.2 MAVS

Mitochondrial antiviral signaling protein (MAVS), also known as interferon-beta promoter stimulator 1 (IPS-1), is a 57 kDa multidomain adaptor protein, that interacts with oligomerized RIG-I to propagate the signal further. MAVS attaches to the RIG-I tetramer, which functions as nucleation point to the MAVS filament, with its N-terminal CARD domain (Figure 5). Although MAVS is attached to the mitochondria by its C-terminal transmembrane domain, its linker domain is long and flexible enough to allow the CARD domain to move around. As more MAVS CARD domains aggregate to the RIG-I tetramer, they start to form a filament. This filament promotes the formation of a scaffolding complex consisting of TNFR-associated death domain (TRADD), Fas-associated death domain (FADD), and a kinase RIP1. (Scott 2010; Wu and Hur 2015)

### 1.11.3 Kinases associated with the RIG-I pathway

TANK-binding kinase 1 (TBK1), also known as T2K, is an important component of many signaling pathways, including the RIG-I pathway. TBK1 phosphorylates IRF3, allowing it to form the dimers to activate IFN production. TBK1 is recruited to the RIG-I pathway

by different scaffolding proteins, which are associated with the MAVS induced scaffolding complex. (Chau et al. 2008; Ahmad et al. 2016)

Inhibitor of nuclear factor kappa-B kinase subunit epsilon (IKK-e) is another kinase that phosphorylates IRF3, with the same outcome as TBK1. It is recruited by the same scaffolding proteins as TBK1. (Chau et al. 2008)

### 1.11.4 Signaling pathway

Binding of RIG-I to the viral RNA allows the 2CARD domain to form oligomers with other activated 2CARDs. The oligomerization can happen with the assistance of ubiquitination or through filaments, which occurs more often with longer dsRNA. Once the RIG-Is have formed a tetramer, they can interact with a membrane bound MAVS. The tetramer resembles a "lock-washer" and acts as a nucleation point to which MAVS can aggregate to with N-terminal CARD domains to form a filament. MAVS filament then recruits several proteins, such as adaptor proteins TRADD, TRAF3, and RIP1, which in turn recruit and activate NEMO/IKK complex. This complex together with TBK1 phosphorylates IRF3 and IRF7, which then form mono- and heterodimers. The dimers are transported to the nucleus, where they bind to their target sequences, activating interferon transcription (Figure 6). (Wu and Hur 2015, Chen et al. 2020)

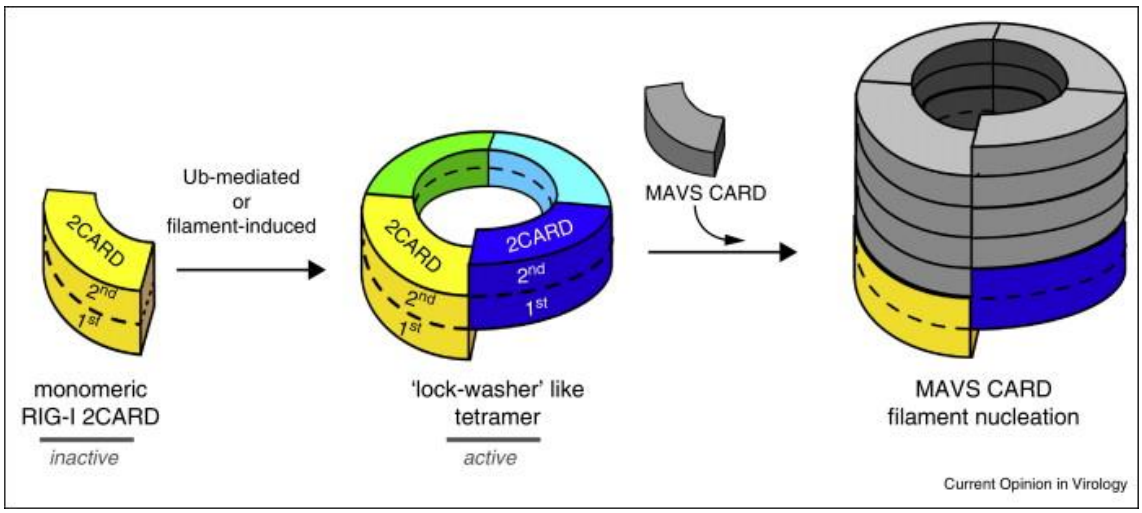


*Figure 5 Proposed model for the assembly of RIG-I tetramer and the subsequent MAVS monomer binding. (Wu and Hur 2015)*

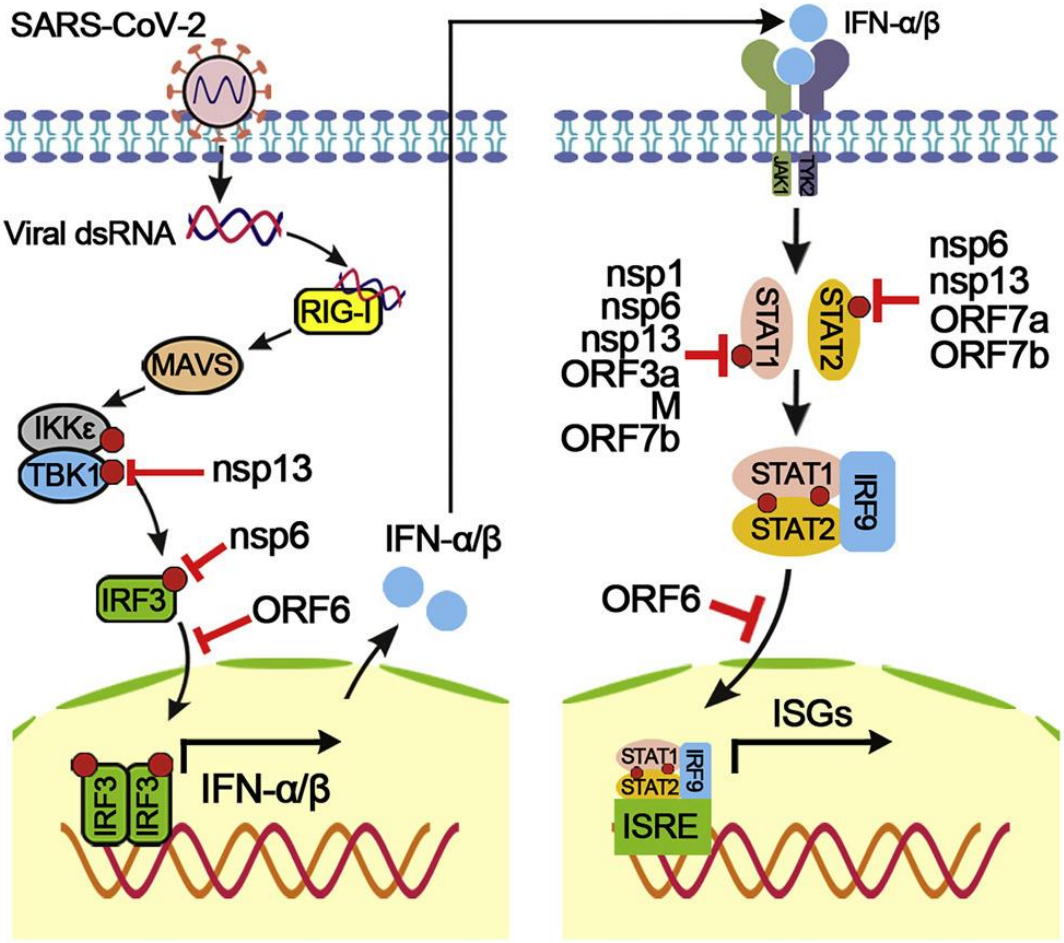


*Figure 6 The RIG-I pathway and JAK-STAT pathway. Left) RIG-I pathway, its components and proposed inhibition targets for some of the SARS-CoV-2 proteins. Right) JAK-STAT pathway, its components and proposed inhibition targets for some of the SARS-CoV-2 proteins. (Xia et al. 2020)*

## 2. Goal of the study

Based on the previous studies of *Coronaviridae* and other viruses in general, it is expected that some of the SARS-CoV-2 proteins will interfere with the host innate immune system to protect the virus from the host antiviral response. These proteins often target pathways regulating interferon gene expression, such as the RIG-I pathway.

The goal of this study was to determine which, if any, of the SARS-CoV-2 proteins interfere with the RIG-I pathway. Additionally, immunogenicity of ORF9B was investigated with SARS-CoV-2 patient serum samples.

## 3. Materials and methods

### 3.1 Plasmids

pcDNA 3.1/Myc-His expression plasmid was used as the backbone plasmids for SARS-CoV-2 proteins and pEBB-N-HA expression plasmid was used for the Zika proteins. pIFN-β- and pIFN-λ1-luc promoter reporter plasmids and RSV-Renilla reporter plasmid were used in the luciferase assays. Delta-RiG-I was expressed with pcDNA 3 expression plasmid.

### 3.2 Sera samples

COVID-19 patient serum samples (n = 119) were collected from 40 patients at Turku University Hospital (TYKS, Turku, Finland; data treated according to ethical permission HUS/1238/2020).

Randomly selected negative control samples (n = 100) were collected in early 2019.

12 samples (3 negative, 4 acute stage, 4 convalescent stage, and 1 positive control) were used in total.

### 3.3 Cell lines

Human embryonic kidney 293 cells (HEK-293) and human hepatocyte-derived carcinoma cells (HuH-7) were the cell lines used in this study. The cell lines were obtained from the cell type collection maintained by the Institute of Biomedicine, University of Turku.

### 3.4 Antibodies

His-tag rabbit Ab (Cell Signaling Technologies), HA-tag mouse mAb (Cell Signaling Technologies), Anti-GAPDH mouse monoclonal IgG (Santa Cruz Biotechnology), Myc-tag rabbit polyclonal IgG (Santa Cruz Biotechnology), Alexa Fluor 488 goat anti-mouse IgG (Invitrogen), Alexa Fluor 488 goat anti-rabbit IgG (Invitrogen), IRDye 680RD Goat anti-rabbit (Licor), IRDye 680RD Goat anti-mouse (Licor). Antibodies were used as per the instructions provided by the manufacturers.

### 3.5 Cell culturing

Cells were handled with aseptic technique in a BSL-2 biosafety cabinet (NordicSafe). Growth media was removed from the cell vessel and cells were washed once with sterile 1 x PBS and detached by adding 5 ml of trypsin-EDTA (MP-Biomedicals). Trypsin was inactivated with 5 ml of growth media (DMEM (BioWhittaker,Lonza), supplemented with, 10% heat-inactivated fetal bovine serum (Invitrogen) , 5% Penicilin/Streptomycin solution (PEST), 5% Glutamax (ThermoFisher)) and cells were thoroughly mixed before being transferred to a new vessel.

### 3.6 Western blotting

Cells were plated on a 6-well plate and transfected at 85-95% confluence with transfection mixture (TransIt (Mirus) or Viafect (Promega), desired plasmid, and OptiMem (ThermoFisher)) and were incubated at 37°C at 5% $CO_2$ 18-24 hours.

The 6-well plate was transferred on ice and the growth media was removed. Cells were washed twice with 500 µl of ice-cold PBS (Medicago) and lysed with 200 µl of ice-cold lysis buffer (0,1% Triton-X, 1x cOmplete Protease Inhibitor Cocktail (Sigma-Aldrich), 50 mM Tris-HCl, 150 mM NaCl, 1% NP-40, 1 mM EDTA, Benzonase nuclease (Sigma-Aldrich)). Lysed cells were scraped with a cell scraper or pipette tip and transferred to 1,5 ml Eppendorf tubes and stored in -80°C for at least 18 hours.

Protein concentrations of the lysates and BSA standards were measured in duplicates with a Bradford assay. BSA standard curve was prepared by diluting BSA to sterile water in different concentrations. 10 µl of diluted lysates and BSA standards were pipetted to a 96-well plate. 200 µl of 5% Bradford reagent was added to each well and the plate was incubated for 5 minutes. Absorbances were measured at 450 nm wavelength with a plate reader (Victor Nivo, Perkin Elmer).

Lysate sample protein concentrations were equalized with sterile water to match the sample with the lowest protein concentration. Sodium dodecyl sulfate (SDS) buffer was added, and samples were boiled for 5 min at 100°C. Boiled samples were loaded to a SDS gel (Any kD Mini-PROTEAN TGX gel, Biorad) submerged to run buffer (1 x TGS) in a gel tank (Mini-PROTEAN Tetra Cell, Biorad) and were ran for 45-60 min at 180 V (PowerPac HC, Biorad). Gel pads and nitrocellulose membrane (GE Healthcare,

Amershan) were soaked in transfer buffer (20% methanol, 25 mM Tris, 192 mM glycine). Proteins from the gel were transferred to a membrane with semi-dry transfer system (Biorad) for 20-25 min at 20 V. Membrane was rinsed with sterile water, and blocked with blocking buffer (5% BSA or non-fat milk/TBS-Tween) for 1 h at RT. Blocking buffer was removed and membrane was washed once with TBS-Tween for 5min, after which primary antibodies diluted to 7,5 ml of blocking buffer were added to the membrane and were incubated o/n at +4°C.

The primary antibody solution was removed and the membrane was washed 3 x 10 min with TBS-Tween. Secondary antibodies diluted in 7,5 ml of blocking buffer were added to the membrane and incubated for 1 h at RT in the dark. The secondary antibody solution was removed and the membrane was washed 3 x 10 min with TBS-Tween and imaged with Odyssey$^{Fc}$ (Licor) at 400 nm and 800 nm wavelength.

### 3.7 Immunofluorescence assays (IFA)

#### 3.7.1 IFA using coverslips

Cells on coverslips were transfected at 75-80% confluence and were incubated o/n at 37°C and 5% $CO_2$. Cells were washed once with 1 x PBS and fixed for 20 min at RT with 4% paraformaldehyde (PFA). PFA was removed and cells were washed twice with 1 x PBS and stored at +4°C.

Cells were permeabilized with block-permeabilization solution (1% BSA, 0,1% Triton X-100 in PBS) for 30 min at RT. Cells were incubated with primary antibodies diluted to block-permeabilization solution for 60 min at RT and then washed for 5 minutes thrice with the block-permeabilization solution. Secondary antibodies diluted in the block-permeabilization solution were added and cells were incubated for 30 min at RT in the dark. 4’,6-diamidino-2-phenylindole (DAPI) diluted 1:5000 in PBS was added to the cells, which were then first washed for 10 min with PBS + 0,1% Triton-X-100 and then washed for 5 min twice with PBS. Coverslips were then dipped in sterile water, excess water was dried, and coverslips were embedded on top of a Prolong Antifade Gold (Invitrogen) droplet on an object glass slide and either imaged with a microscope (Leica DMLR) or stored at + 4°C.

### 3.7.2 IFA in immunogenicity assays

10 000 Huh7 cells/well were plated on a 96-well plate and grown o/n at 37°C and 5% $CO_2$. Transfection mixture (200 ng of SARS-CoV-2 S1 or Orf9B, 0,15 µl of TransIt (Mirus) in OptiMem (ThermoFisher)) was prepared and incubated for 25 min. 10 µl of transfection mixture or OptiMem was added per well and cells were incubated o/n) at 37°C and 5% $CO_2$.

Cells were fixed with 4% PFA for 20 min at RT. PFA was removed,1 x PBS was added, and cells were stored at +4°C.

Cells were permeabilized with 0,1% Triton-X-100 + PBS for 5 min at RT and then labeled with mouse monoclonal anti-His antibodies (Cell Signaling Technologies) diluted 1:200 and serum samples diluted 1:40 in 3% BSA + PBS for 1 hour at RT. Serum samples were added in duplicates. Cells were washed for 5 min thrice with 0,5% BSA + PBS and secondary antibodies (1:1000 goat-anti-human A-488 (Licor), 1:1000 goat-anti-mouse A-566 (Licor)) and 1:5000 DAPI were added. Cells were washed for 5 min thrice with 0,5% BSA + PBS, leaving the last wash in the well, and imaged the cells with microscope (Evos, ThermoFisher).

### 3.8 Luciferase assays

96-well plate was seeded with HEK-293 cells at low density and incubated o/n at 37°c, at 5% $CO_2$. Cells at 50% confluence were transfected with 3 ng, 10 ng, and 30 ng of target plasmids or control plasmid, 30 ng of of delta-RIG-I for interferon response induction, 20 ng of reporter gene construct and 50 ng of RSV-Renilla for normalization. Transfection mixtures were incubated for 15-30 min before adding them to the cells. Cells were incubated o/n at 37°C, at 5% $CO_2$.

Growth media was aspirated and wells were washed once with PBS and cells were lysed by adding 20 µl of lysis buffer (TwinLite) and incubating for 15 min at RT on a shaker. 100 µl of FireLite+ (TwinLite) was added per well and mixed gently by pipetting up and down couple of times, after which firefly luciferase values were measured with a plate reader (Victor Nivo, Perkin Elmer). 100 µl of RenLite+ (TwinLite) was added per well and mixed gently by pipetting up and down couple of times, after which Renilla luciferase values were measured with a plate reader (Victor Nivo, Perkin Elmer).

Firefly luciferase values were normalized with Renilla values.

### 3.9 Cloning

#### 3.9.1 Infusion cloning

Backbone plasmids were linearized and dephosphorylated by incubating the plasmids with a digestion mixture (FastDigest BamHI, 10 x FastDigest Green Buffer, nuclease-free $H_2O$) for at least 3 hours.

Target sequences were amplified with PCR. PCR reaction mixture (100 ng of DNA template, 1 x CloneAmp HiFI PCR premix (TakaraBio), 7,5 pmol of forward and reverse primers, filled to 25 µl with nuclease-free $H_2O$) was incubated in thermal cycler (T100 Thermal Cycler, Biorad) at 98°C for 5 min, then cycled 30 times at 98°C for 10 sec, at 55°C for 15 sec and at 72°C for 60 sec/kb. Final extension was at 72°C for 5 min.

Digested plasmids and PCR products were loaded to an 1,5% agarose gel and ran for 1,5 h at 100 V (PowerPac HC, Biorad) in TAE buffer (40 mM Tris base, 20 mM acetic acid, 1 mM EDTA) in an agarose gel electrophoresis (AGE) chamber (HU15 mini horizontal, Scie-Plas). Gel parts containing the linearized plasmids were localized with UV light, excised, and purified or stored in +4°C.

DNA was purified with a gel purification kit (NucleoSpin, Machney-Nagel).

Cloning reaction mixture (100 ng of purified PCR product, 100 ng of linearized backbone plasmid, InFusion enzyme premix (TakaraBio), filled to 10 µl with deionized $H_2O$) was incubated at 50°C for 15 min and then placed on ice. Stellar Competent cells (TakaraBio) were thawed on ice right before use. 50 µl of cells were incubated with 2,5 µl of reaction mixture for 30 min on ice after which the cells were heat shocked for 45 sec at 42°C and then transferred back on ice for 2 min. SOC media warmed to 37°C was used to fill the cell tubes to 500 µl, which were then incubated by shaking at 200 rpm for 1 h at 37°C. 1:10 of cell mixture was plated and the rest was centrifuged at 1500 x g for 5 min. Supernatant was discarded, the cell pellet was resuspended to 100 µl of SOC media and then plated on LB plates, which were incubated 18-22 hours at 37°C.

Colonies from the plates were picked and grown in 4 ml of culture media (Luria broth + antibiotics (gentamycin or ampicillin)) o/n at 37°C. Glycerol stocks (500 µl of culture,

50% glycerol) were prepared and stored at -80°C. Plasmids were purified from the cultures with a miniprep kit (GeneJet plasmid miniprep kit, ThermoFisher).

Sequencing samples (400-500 ng of purified plasmid, primer (5 pmol), filled to 10 µl with nuclease-free $H_2O$) were prepared and sent for sequencing to GeneArt.

After confirming that the sequences were correct, new cultures were prepared from glycerol stocks or stored cultures. Cultures were grown in LB + antibiotics (gentamycin or ampicillin) o/n at 37°C and 210 rpm, after which plasmids were extracted and purified with a maxikit (Endofree plasmid maxi kit, Qiaqen).

DNA concentration and its purity were determined with NanoDrop (DeNovix).

### 3.9.2 Restriction enzyme digestion and plasmid isolation

Target and backbone plasmids were digested by incubating them in a digestion mixture (1,5 µg of plasmids, 1 x FastDigest Green buffer, FastDigest BamHI, filled to 20 µl with nuclease-free $H_2O$) at 37°C for 1 h. Digested samples were loaded to 0,8% agarose gel and ran for 1 h at 95 V (PowerPac HC, Biorad) in TAE buffer (40 mM Tris base, 20 mM acetic acid, 1 mM EDTA) in an AGE chamber. Gel parts containing the linearized plasmids were localized with UV light, excised, and purified or stored in +4°C.

Plasmids were purified with gel extraction kit (NucleoSpin, Machney-Nagel).Purified, linearized insert plasmids were ligated with linearized backbone by incubating them in a ligation mixture (1 x T4 ligase, FastDigest buffer, insert DNA, backbone DNA, fill to 10 µl with nuclease-free $H_2O$) o/n at +4°C.

Competent DH5a cells were thawed on ice, after which 30 µl aliquotes of them were mixed with ligated plasmids and then incubated on ice for 30 min. Cells were heat shocked for 50 seconds at 42°C and incubated on ice for 2 minutes. 700 µl of LB was added per tube, and incubated on a shaker at 37°C, at 210 rpm for 1 h. Cells were plated on agar plates (LB, antibiotics (gentamycin or ampicillin) and were incubated at 37°C o/n. Colonies were picked and grown in 4 ml cultures (LB, antibiotics (gentamycin or ampicillin) at 37°C o/n.

Glycerol stocks (500 µl of culture, 50% glycerol) were prepared and stored at -80°C. Plasmids were purified from the cultures with a miniprep kit (GeneJet plasmid miniprep kit, ThermoFisher).

Sequencing samples (400-500 ng of purified plasmid, primer (5 pmol), filled to 10 µl with nuclease-free $H_2O$) were prepared and sent for sequencing to GeneArt.

After confirming that the sequences were correct, new cultures were prepared from glycerol stocks or stored cultures. Cultures were grown o/n at 37°C and 210 rpm, after which plasmids were extracted and purified with a maxikit (Endofree plasmid maxi kit, Qiaqen).

DNA concentration and purity were determined with NanoDrop (DeNovix).

## 4. Results

### 4.1 Expression of SARS-CoV-2 proteins

To perform the luciferase assays it was first necessary to produce and purify several plasmids with the target gene sequence, and to verify their expression in the cell lines with Western blotting (WB) and immunofluorescence assays (IFA).

WB is a very common technique that is used to determine if the protein of interest is present in the sample. The sample is taken from a cell lysate and proteins are separated by weight with SDS-PAGE electrophoresis. Proteins are transferred to a membrane and visualized with fluorescent-labelled antibodies.

IFA is another commonly used technique that is used to visualize target proteins within the cell, providing information of the expression and cellular location of the proteins. After transfecting the cells with an expression plasmid containing the target protein, the expressed proteins are labeled with antibodies and visualized with a fluorescent microscope.

The expression of control proteins, Zika virus non-structural proteins (ZIKV NS) 1, 3, and 5, were done with the previously used pEBB-N-HA expression plasmids. The pEBB-N-HA plasmids had been used previously in the same lab to express several different Ebola and Zika virus proteins, that were subsequently biologically active and produced reliable data in luciferase assays. Expression of ZIKV NS proteins was successfully confirmed with both IFA and WB. SARS-CoV-2 proteins on the other hand proved to be more challenging to express.

The first attempt to express SARS-CoV-2 nonstructural proteins was done using the same pEBB-N-HA backbone as with the ZIKV NS and structural SARS-CoV-2 proteins (E-, N-, M- and S-proteins). The plasmids containing the structural SARS-CoV-2 genes had already been produced by other lab members and S-, M- and, N- proteins had been successfully expressed before the start of this study. To verify this, their expression was analyzed again with IFA and WB, yielding good expression levels for N-, M- and S-proteins, but not for E-protein (Figures 7, 8, and 9).

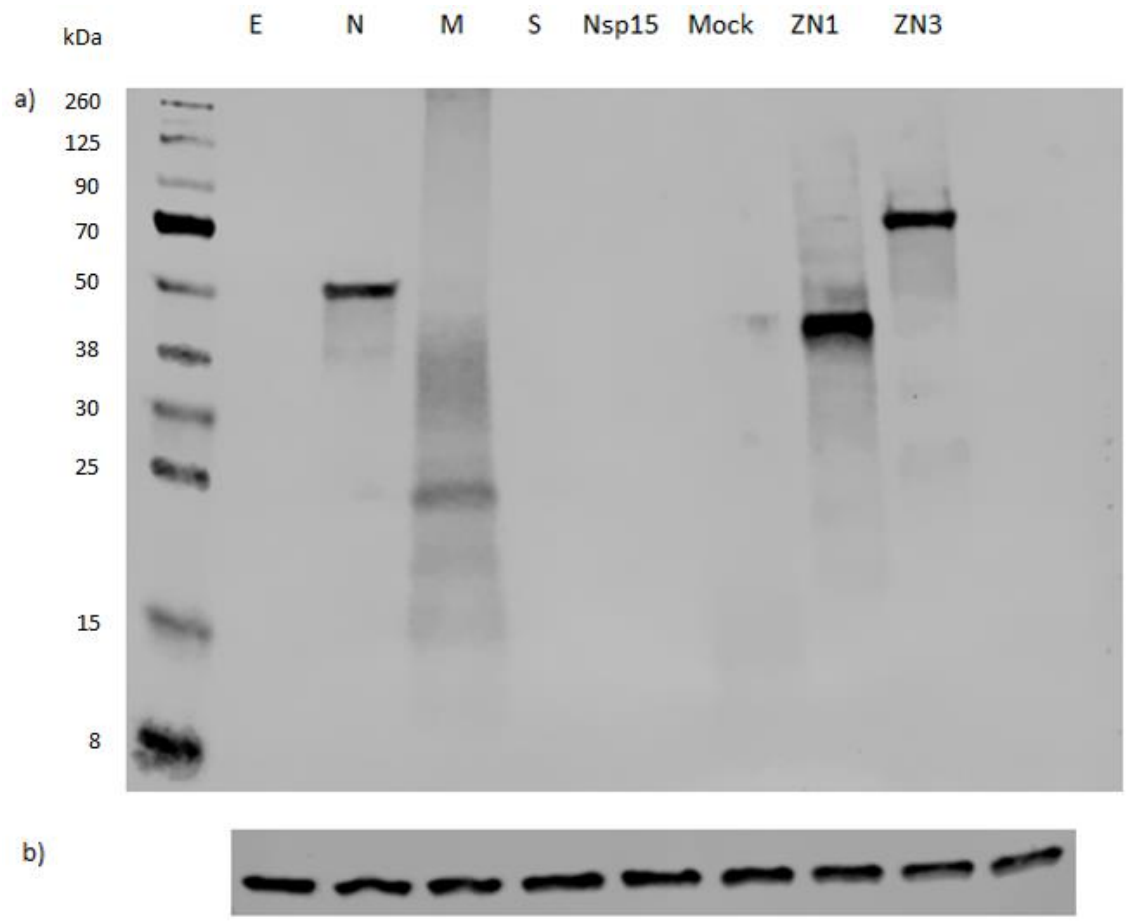


*Figure 7 HEK-293 cells on 6-well plates were transfected with 2,4 µg of SARS-CoV-2 structural protein or one of the control Zika non-structural expression plasmids. A mock well with no plasmids was used as a baseline control. After incubating overnight, cells were lysed and ran in a gel at 180 v for 40 min, after which they were transferred on to a nitrocellulose membrane with semi-dry transfer. The membrane was blocked with 5% fat-free milk/TBST for 1 hour and then incubated overnight in a spinning rack at +4c with primary antibodies. Membrane was stained the next day with secondary antibodies and imaged with Odyssey. a) SARS-CoV-2 structural proteins along with the controls b) GAPDH controls with the same lysates as in a).*

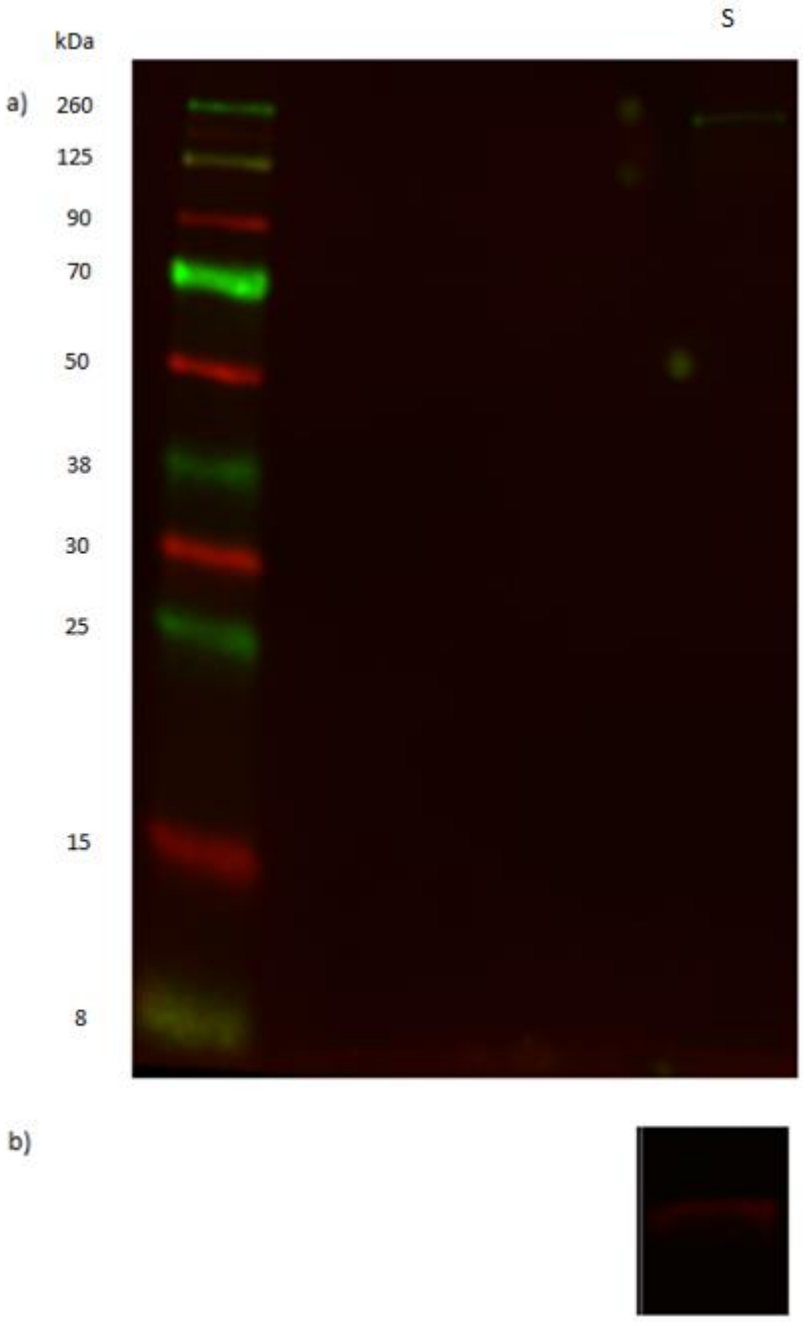


*Figure 8 HEK-293 cells on 6-well plates were transfected with 2,4 µg of SARS-CoV-2 structural protein or one of the control Zika non-structural expression plasmids. After incubating overnight, cells were lysed and ran in a gel at 180 v for 40 min, after which they were transferred on to a nitrocellulose membrane with semi-dry transfer. The membrane was blocked with 5% fat-free milk/TBST for 1 hour and then incubated overnight in a spinning rack at +4c with primary antibodies. Membrane was stained the next day with secondary antibodies and imaged with Odyssey. a) SARS-CoV-2 S protein b) GAPDH control with same lysate as in a).*

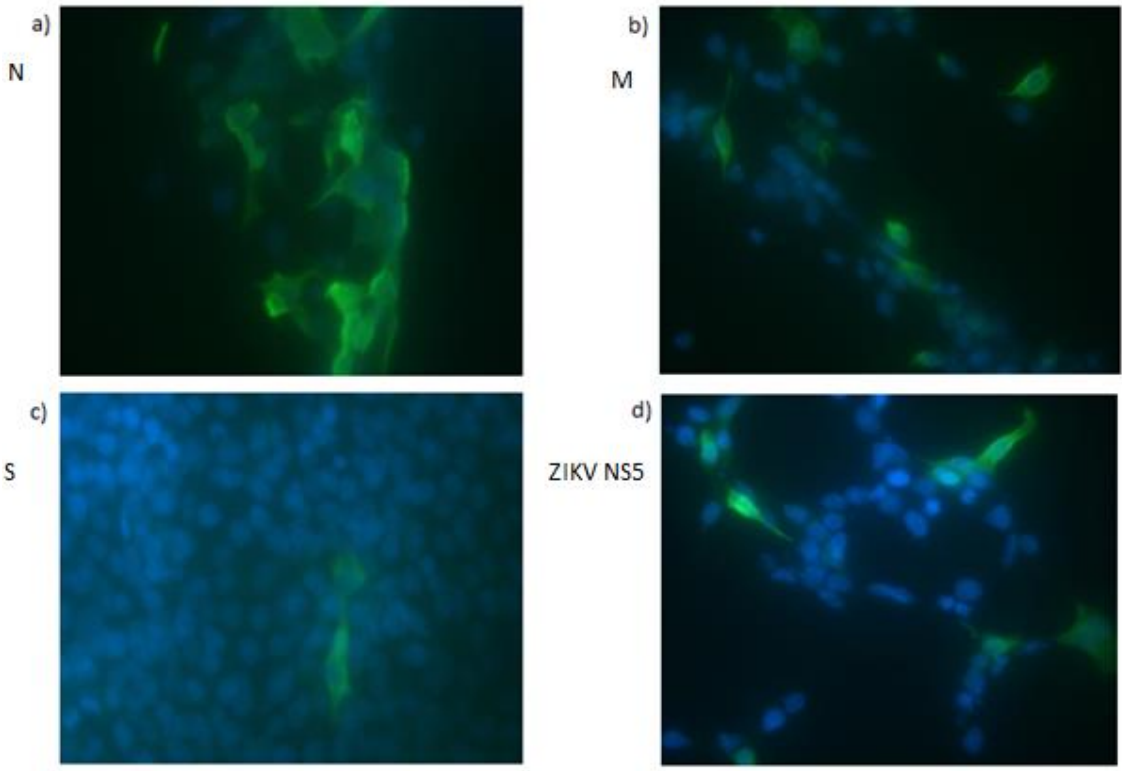


*Figure 9 Huh7 cells plated on a 12-well plate with glass coverslips were transfected with 1000 ng/well of a given SARS-CoV-2 structural protein or control expression plasmids followed by labeling with fluorescent antibodies. Green color indicates the proteins that have been detected by the anti-HA antibodies. Blue color indicates the cell nuclei stained by DAPI a) SARS-CoV-2 N-protein b) SARS-CoV-2 M-protein c) SARS-CoV-2 S-protein d) ZIKA virus NS5-protein*

Most of the non-structural SARS-CoV-2 proteins were visible in the IFA, but none of them could be seen in WB, despite repeating the runs multiple times and with adjustment to the run and incubation conditions.

The failure to express target proteins when their sequence was inserted to pEBB-N-HA prompted us to use a different expression plasmid. The expression plasmid pcDNA 3.1/myc-His was chosen because it had also been used to successfully with similar mammalian cell models to express many proteins in the same lab. The inserts from the previous expression plasmids were transferred to the expression plasmids first with classical restriction enzyme method. However, after the plasmids created in this manner yet again failed to express any proteins, a new, next generation cloning method called Infusion cloning was used. Infusion cloning does not utilize ligases at all, is very accurate, and very rarely introduces errors to the insert sequence. However, despite the efficiency of the cloning method, plasmid constructs produced via this

manner also failed to express any of the SARS-CoV-2 non-structural proteins, despite having their sequences confirmed as correct by sequencing.

Since switching plasmid and the cloning method failed to resolve the expression problem, a new approach had to be used. It was decided to use codon-optimized insert sequences, which were cloned into the pcDNA 3.1/myc-His backbone plasmid by the same company doing the codon optimization (Gene Universal). These ready-made plasmid constructs were then produced and purified with the same methods as the previous constructs and used to transfect cells. As a result, SARS-CoV-2 proteins Nsp1 and 14 were clearly expressed as shown in the WB assay (Figure 10). SARS-CoV-2 non-structural proteins Nsp6 and Nsp13 did not seem to be expressed, although the lane with the Nsp6 sample did have a band that was stained with His- antibodies. However, the location of this band did not correspond to the size of Nsp6 (Figure 10).

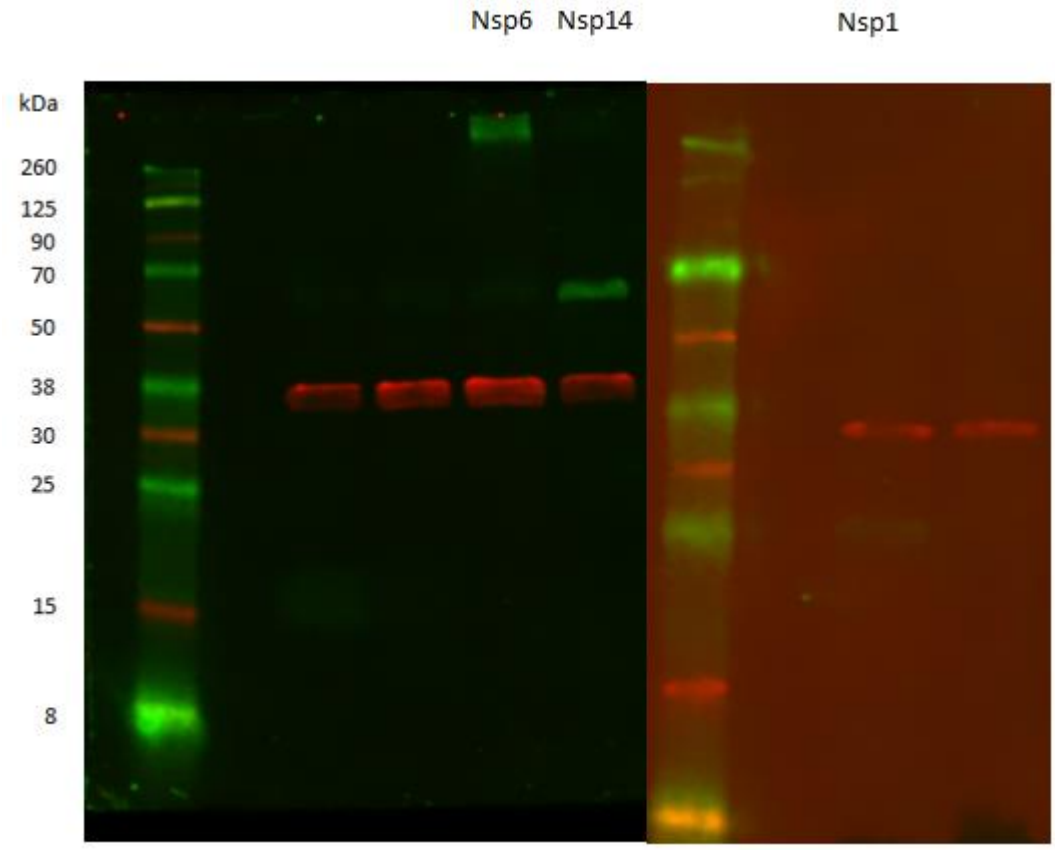


*Figure 10 Hek-293 cells on 6-well plates were transfected with 2,4 µg of SARS-CoV-2 structural proteins or one of the control Zika non-structural expression plasmids. After incubating overnight, cells were lysed and ran in a gel at 180 v for 40 min, after which they were transferred on to a nitrocellulose membrane with semi-dry transfer. The membrane was blocked with 5% fat-free milk/TBST for 1 hour and then incubated overnight in a spinning rack at +4c with primary antibodies (anti-His, anti-GAPDH). Membrane was stained the next day with secondary antibodies and imaged with Odyssey.*

The successful expression of almost all SARS-CoV-2 proteins of interest allowed to proceed with luciferase assays.

### 4.2 SARS-CoV-2 structural proteins do not inhibit the RIG-I pathway

Luciferase assay is a reporter system that is used to study different cellular functions, such as signaling pathways, in the eukaryotic cells. It utilizes two reporter plasmids: an experimental reporter plasmid, which has a firefly luciferase enzyme-coding gene downstream of the promoter of the gene of interest, and a control reporter plasmid which contains renilla luciferase enzyme-coding gene downstream of the constantly active promoter. The latter is used to provide a baseline luciferase activity based on transfection efficiency. Since the assay uses two different luciferases that produce luminescence in the presence of different substrates, this combination makes it possible to normalize the results and thus to eliminate variations arising from different sources, such as pipetting errors or differences in cell amounts.

In this study, Promegas' Dual-Luciferase Reporter Assay System was used, which can detect firefly (*Phonitus phyralis*) and Renilla (*Renilla reniformis*) luciferases as experimental and control luciferases, respectively. The reporter plasmids used in this study had IFN-λ promoter in front of the firefly luciferase gene and a constitutively active Rous sarcoma virus promoter in front of Renilla luciferase gene.

To study the effects of SARS-CoV-2 proteins on the RIG-I-pathway, HEK-293 cells were transfected with a plasmid containing a protein of interest or control protein, both luciferase gene-containing plasmids, and a constitutively active delta-RIG-I to induce the pathway. As shown in Figure 11, delta-RIG activates the RIG-I pathway efficiently, leading to the activation of IFN-λ promoter and subsequent luciferase expression, detected by luminescence (Figure 11, indicated by C+). Expression of NS3/4A protein of hepatitis C virus resulted in almost no luciferase signal, as expected since NS3/4A cleaves MAVS on the RIG-I pathway, fully inactivating the pathway (Li et al. 2005). The mock cells resulted in baseline signals from both luciferases. Cells expressing SARS-CoV-2 structural proteins S, E, N, and M, did not inhibit the RIG-I substantially when compared to the positive control.

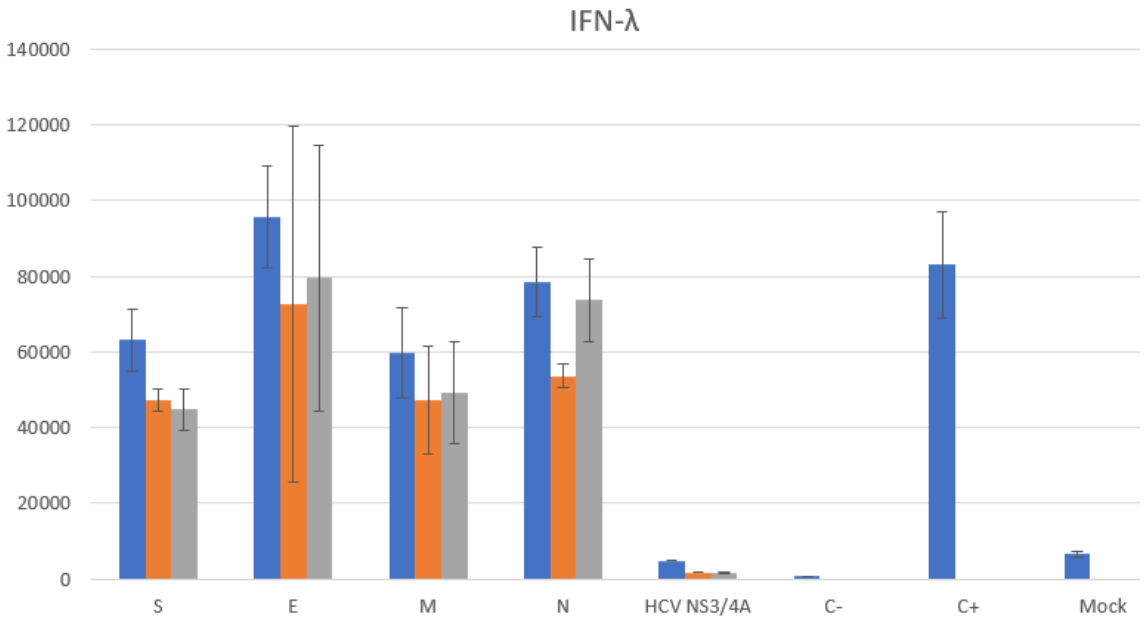


*Figure 11 Normalized luciferase signals from SARS-CoV-2 structural proteins. HEK-293 cells were plated on 96-well plate, and transfected with 3 ng, 10 ng and 30 ng per well of either SARS-CoV-2 structural proteins (S, E, M, N) or HCV NS3/4A expression plasmids. Cells were also transfected with 50 ng of Renilla, 30 ng of delta-RIG-I and 20 ng of IFN-lambda-promoter luciferase per well, with the exception of the negative control (C-), which only had the reporter plasmids, the positive control (C+), which had only delta-RIG-I and the reporter plasmids, and mock cells, which were not transfected with any plasmids. Cells were lysed after overnight incubation and the luminescence was measured. Assay was done once with three replicates within assay.*

### 4.3 SARS-CoV-2 Nsp1, Nsp6 and Nsp13 inhibit the activation of IFN-λ promoter

Although the expression of Nsp1 and Nsp14 was confirmed with the WB:s, their inhibitory effects, or their lack of, had to be first tested with a promoter that was known to be inhibited by them. Since the effects of many SARS-CoV-2 non-structural proteins on the type I interferon pathways are known, a reporter plasmid with IFN-β promoter and luciferase reporter gene was used to assess if the non-structural proteins we had produced would have similar effects on the RIG-I pathway as suggested by existing literature. Nsp1 inhibited the RIG-I pathway, shutting it off completely, while Nsp14 had no effect on the pathway (Figure 12).

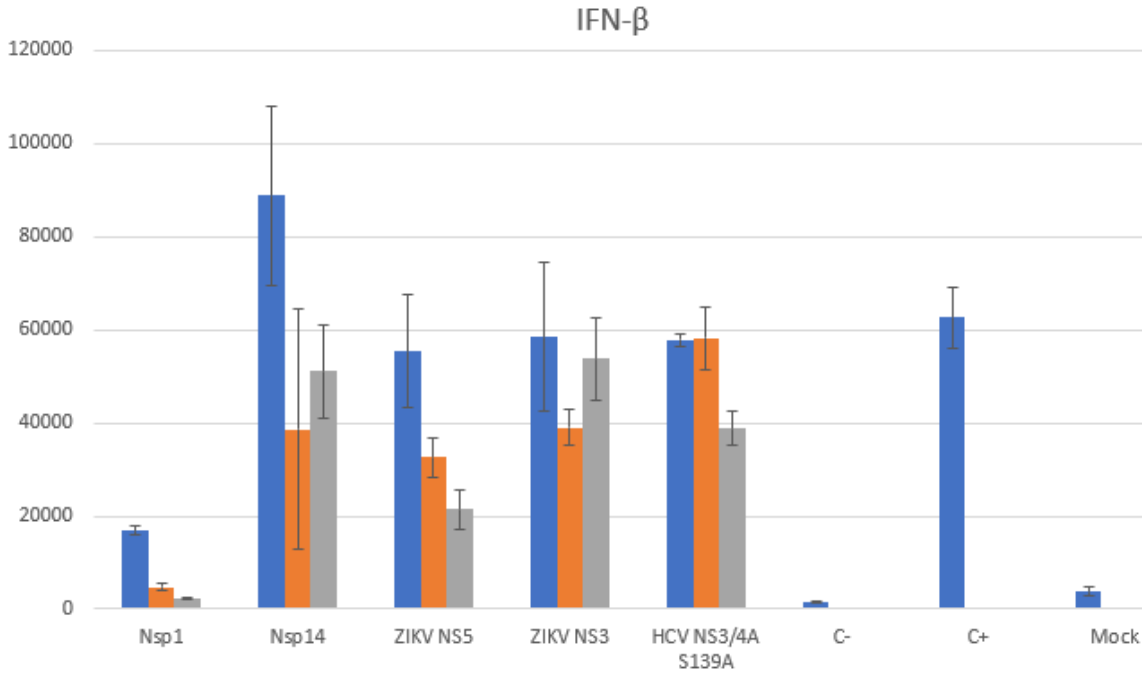


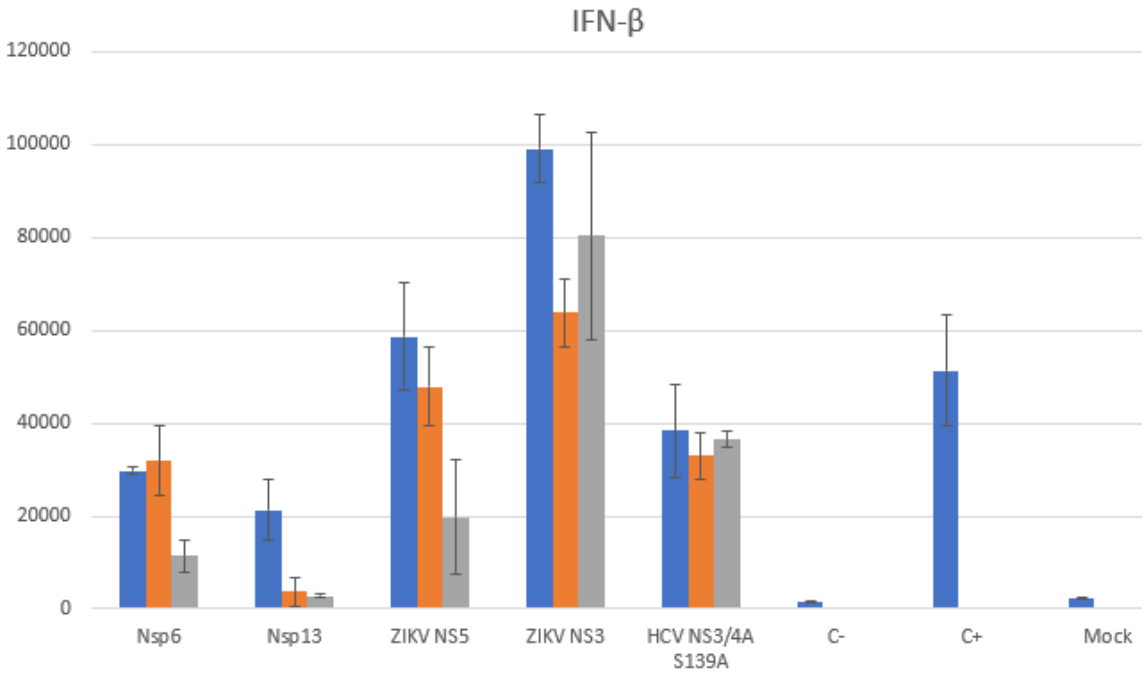


*Figure 12 Normalized luciferase signals from SARS-CoV-2 non-structural proteins 1,6,13 and 14. HEK-293 cells were plated on 96-well plate, and they were transfected with 3 ng, 10 ng and 30 ng per well of either NSPs, Zika NSPs or HCV NS3/4A S139A expression plasmids. Cells were also transfected with 50 ng of Renilla, 30 ng of delta-RIG-I and 20 ng of IFN-β-promoter luciferase per well, with the exception of the negative control (C-), which only had the reporter plasmids, the positive control (C+), which had only delta-RIG-I and the reporter plasmids, and mock cells, which were not transfected with any plasmids. Cells were lysed after overnight incubation and the luciferase values were measured. Assay was done once.*

The inhibitory effect of Nsp1 was very strong, inhibiting the pathway even more efficiently than the HCV NS3/4A would. In this assay, HCV NS3/4A did not inhibit the signal, since a S139A mutant was used. The signal strength gained from the Nsp14 was slightly higher than the signal strength of the positive control. Mock wells showed only baseline signal. The assay was done only once with the IFN-β promoter construct.

After confirming the target proteins produced by our lab had inhibitory capabilities as suggested by the existing literature, the next phase of luciferase assays was started. Instead of the IFN-β promoter, it was replaced with an IFN-λ1, also known as IL-29, promoter. Otherwise, the assay remained unchanged. Even though the expression of Nsp6 and Nsp13 could not be confirmed with either WB or IFA, they were still included to the assay, as they could still prove to be informative if they had any inhibitory effects. Like with IFN-β promoter, Nsp1 completely shut off the RIG-I pathway, again silencing the pathway more efficiently than HCV NS3/4A. Likewise, Nsp14 had similar effect with IFN-λ1 as IFN-β, not inhibiting the signal strength. Surprisingly, Nsp6 and 13 both reduced the firefly luciferase signal to a significant extent, with Nsp6 being the more efficient one. (Figure 13).

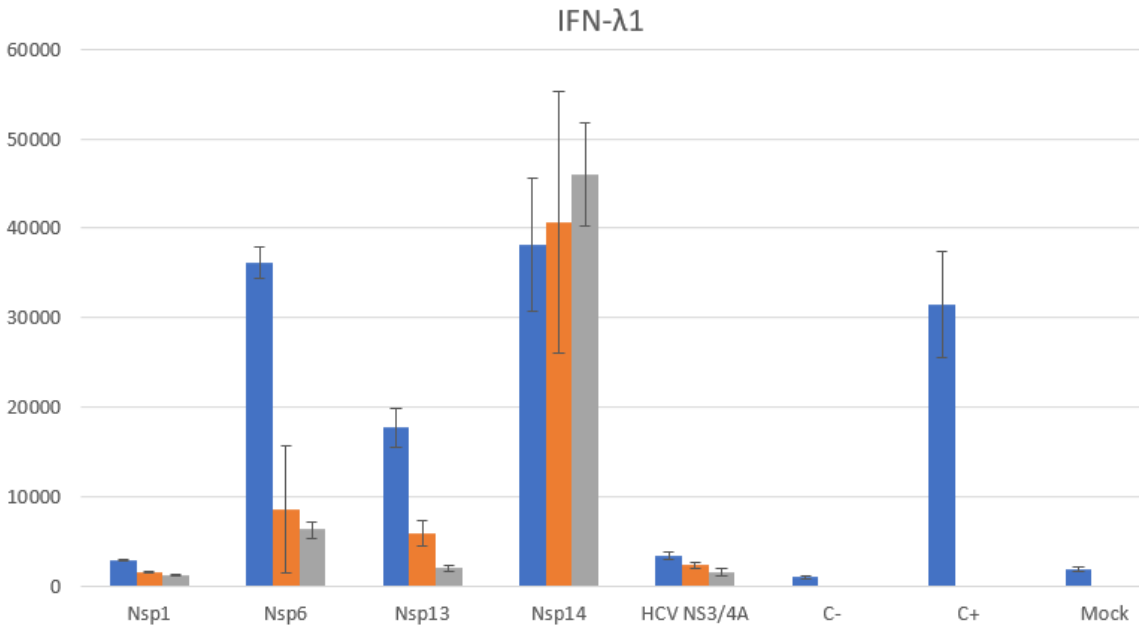


*Figure 13 Normalized luciferase signals from SARS-CoV-2 non-structural proteins 1,6,13 and 14. HEK-293 cells were plated on 96-well plate, and they were transfected with 3 ng, 10 ng and 30 ng per well of either NSPs or HCV NS3/4A expression plasmids. Cells were also transfected with 50 ng of Renilla, 30 ng of delta-RIG-I and 20 ng of IFN-λ1-promoter luciferase per well, with the exception of the negative control (C-), which only had the reporter plasmids, the positive control (C+), which had only delta-RIG-I and the reporter plasmids, and the mock cells, which were not transfected with any plasmids Cells were lysed after overnight incubation and the luciferase values were measured. Assay was done three times.*

Like before, HCV NS3/4A silenced the signal efficiently, and the negative and positive controls behaved as expected. The assays were repeated thrice, with triplicates for each protein, and each run produced similar results. Inhibitory effects were statistically significant.

### 4.4 SARS-CoV-2 ORF9B protein is not immunogenic

Immunogenic viral proteins are of great interest to vaccine development since they can be used as the immunizing component in recombinant and other vaccine types. To investigate whether SARS-CoV-2 ORF9B was one of such proteins, the protein was expressed in cells and COVID-19 patient sera was used as primary antibody in IFA to study if sera contain antibodies detecting ORF9B protein.

The expression of ORF9B was first investigated with an IFA using antibodies detecting HA-tag. As seen in Figure 14, Huh7 cells expressed ORF9B in significant amounts.

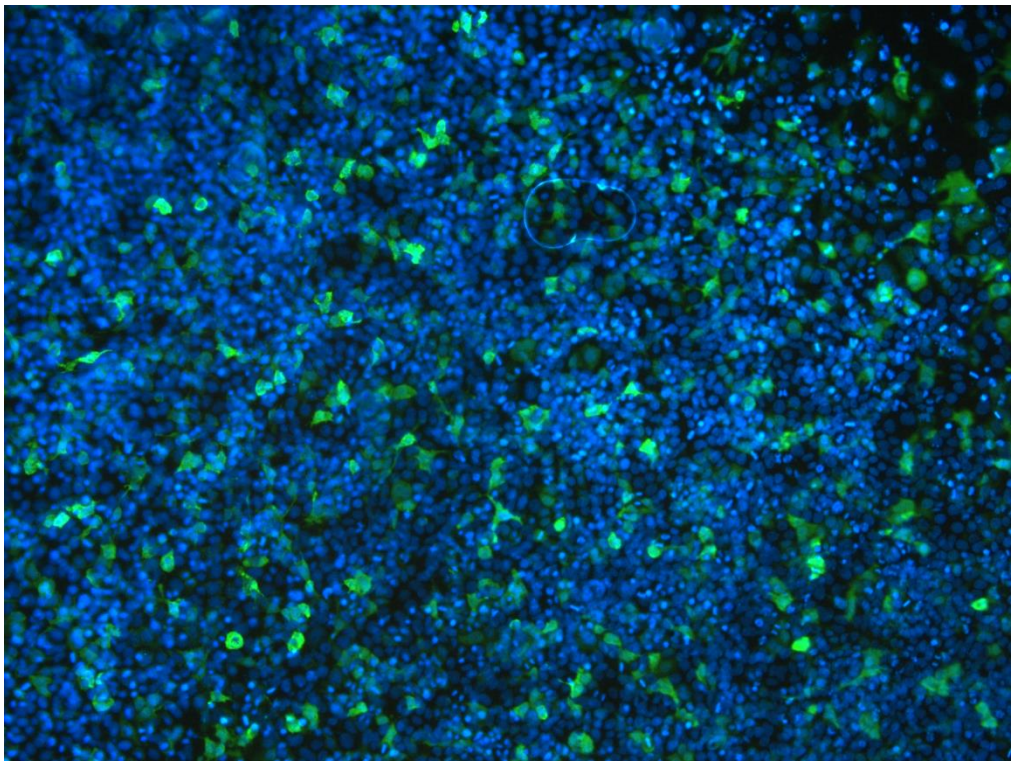

*Figure 14 Huh7 cells transfected with expression plasmid encoding SARS-CoV-2 ORF9B protein. The bright green color marks the location of ORF9B detected with anti-HA antibodies. The blue color indicates cell nuclei stained by DAPI. ORF9B is clearly expressed in approximately 30% of the cells.*

The immunogenic properties of ORF9B were investigated with IFA assay in which Huh7 cells were transfected with either SARS-CoV-2 ORF9B or S1 in pcDNA 3.1/myc-His expression plasmid. A plasmid containing the sequence for the S-protein domain S1 was used as a protein control for immunogenicity. Cells expressing the proteins were incubated with different sera samples taken from humans at different stages of SARS-CoV-2 infection. These sera samples were either from negative, convalescent, or acute stages of the illness, and also included a positive sample as a control. All sera samples had been heat-inactivated prior to the assay to ensure safe handling in BSL-2 laboratory. The positivity of samples to the presence of viral genome from SARS-CoV-2 had been determined beforehand with a PCR test

The results of the IFA indicated that ORF9B was not immunogenic, regardless of what serum sample type was used. One positive control, four convalescent stage samples, four acute stage samples, and three negative samples were used. An example of IFA with two sera is shown in Figure 15. None of the cells expressing SARS-CoV-2 ORF9B showed any staining with anti-human IgG secondary antibodies, while the expression of ORF9B was clearly visible with antibodies detecting the HA-tag of the ORF9B. The cells transfected with the S1-domain appeared immunogenic with three convalescent samples. None of the negative serum samples and mock cells were recognized by patient sera, indicating the lack of false positives.

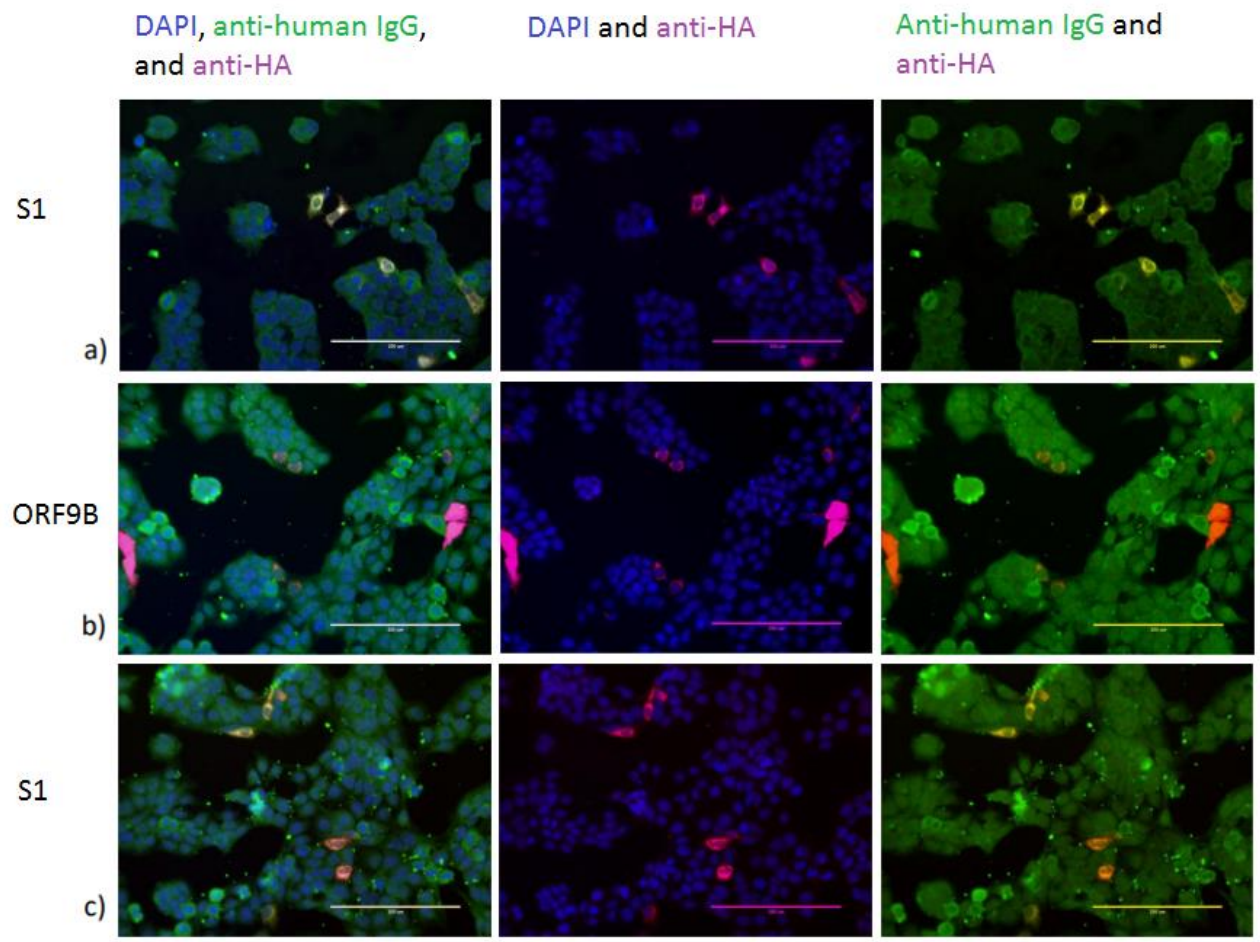


*Figure 15 Huh7 cells incubated with human sera from various patients. Bright green color indicates cells to which antibodies in the patient samples have bound. Purple color indicates cells transfected with either SARS-CoV-2 ORF9B or S1. Blue color indicates cell nuclei stained by DAPI. a) Positive control serum and SARS-CoV-2 S1 b) Convalescent serum and SARS-CoV-2 ORF9B C) Convalescent serum and SARS-CoV-2 S1*

## 5. Discussion

While the expression of target proteins proved to be a more difficult, longer, and frustrating endeavor than anticipated, it provided valuable lessons in protein expression.

Even though the expression of SARS-CoV-2 Nsp6 and Nsp13 was not detected in either IFA or WB, the conformation of the expression of protein of interest is not always necessary, or even possible. Due to its small size (10,8 kDa), the ORF9B protein was very difficult to visualize with WB. Although other research groups have managed to successfully visualize SARS-CoV-2 non-structural proteins and ORFs, they have used a different expression plasmid, pGAGS being the most common (Gordon et al. 2020). Since this expression plasmid was not available for this study, luciferase assays were performed without knowledge on expression levels of SARS-CoV-2 Nsp6 and Nsp13 proteins. However, the difficulties in expression were unlikely related to the expression plasmids in use since these have worked perfectly fine with other inserts. In addition, the sequences of plasmid constructs were all correct. Also, the cells, transfection, cell lysate collection, and WB methods were not the sources of negative results, as all the controls were successfully detected every time. It is possible, that the non-optimized constructs could have been toxic to the cells, destroying any successfully transfected cells, or that the proteins were expressed at such a low level that the WB and IFA were not sensitive enough to detect them. Also, due to a lack of influence from other viral proteins that are normally present during infection, proteins of interest could have been folded or processed incorrectly. Semi-dry transfer during WB is another possible reason for not detecting the SARS-CoV-2 Nsp6 and Nsp13 proteins since this method is not as efficient as wet transfer.

The success in expression of SARS-CoV-2 Nsp1 and Nsp14 proteins with codon-optimized inserts gives a compelling argument for the standardized use of codon-optimization whenever it is possible. Since the proteins are already produced in an abnormal state when transfecting cell cultures with plasmids, compared to *in vivo* situations in infection, the different nucleotide sequence does not affect functions of the protein, as long as the primary amino acid sequence remains the same between codon-optimized and non-optimized proteins. In many labs that have successfully

expressed SARS-CoV-2 proteins, this is already a standard practice (Gordon et al.2020; Lei et al. 2020).

The lack of any inhibitory effect on the IFN-λ-promoter by SARS-CoV-2 S-, E-, N- and M proteins was in line with previous studies. Although the M protein had been previously demonstrated to inhibit type-I interferon production, it does so by phosphorylating STAT1, rather than by interfering with any of the RIG-I pathway components (Lei et al. 2020; Xia et al. 2020). Except for the E-protein, all SARS-CoV-2 structural proteins were successfully expressed in both IFA and WB (Figures 5, 6, and 7). Although at first glance the expression of S-protein appears to be weak, the faint loading control on the same lane indicates that the loaded protein amount, or the amount of cells before lysing, was lower than intended. The expression of E-protein was not expected to be seen with either WB or IFA, as other lab members in the same lab had failed to express the E-protein using the same expression plasmid. However, at least in one study (Gordon et al. 2020) E-protein was successfully expressed, albeit by using a different expression vector, pLVX-EF1alpha-IRES-Puro, which additionally had a 2 x Strep-tag instead of the HA-tag used in the SARS-CoV-2 structural protein constructs in this study.

The inhibitory effect of Nsp6 and Nsp13, despite their absence in WB and IFA, on the RIG-I pathway was in line with previous studies (Lei et al. 2020; Xia et al. 2020). However, in these previous studies on type I interferon inhibition had been studied. The fact that SARS-CoV-2 Nsp6 and Nsp13 also inhibit the IFN-λ promoter sheds light into the multiple functions that these proteins might harbor. Regarding the WB and IFA, unlike ORF9B, both of them are large enough to be seen on WB, so their size should not be the issue. It might be possible that the His-antibodies used simply didn’t recognize these constructs, for example because of their altered tertiary structure due to the inclusion of His-tag region. However, this seems unlikely since His-tag is a relatively small tag. In the case of Nsp6, there is also the question of line that can be seen in the stacking gel. Despite sonicating and repeating runs, this line was always present, and was always stained by the His-antibodies. It could be the Nsp6 protein, albeit in an aggregate form or similar structure that has immense difficulty moving through the SDS-PAGE gel.

Of note, when performing the luciferase assay with the IFN-β-luciferase construct, the HCV NS3/4A surprisingly did not inhibit the luciferase signal at all. Upon further investigation, it was noticed that a wrong variant of the protein had been used: a clone which had a S139A mutation that deleted the protein's inhibitory activity.

The inhibitory activity of SARS-CoV-2 Nsp1 on the RIG-I pathway was expected. Recent studies (Lei et al. 2020; Xia et al. 2020) have indicated that Nsp1 has an inhibitory effect on the RIG-I pathway leading to reduced activation of IFN-β promoter. However, the magnitude of this inhibitory effect was surprising. Nsp1 inhibitory effect exceeded even the inhibitory effect of HCV NS3/4A, which interferes with the RIG-I pathway by directly cleaving MAVS (Li et al. 2005). Further assays with different RIG-I pathway components, such as MAVS and IKKe, are required to determine which part of the RIG-I pathway Nsp1 inhibits. It also would be interesting to see if Nsp1 inhibits the RIG-I pathway indirectly by shutting down the host cell translation.

Contrary to the other SARS-CoV-2 Nsps in this study, Nsp14 did not show any inhibitory effect on the RIG-I pathway. Instead, Nsp14 seemed to slightly elevate the activity of IFN-β and IFN-λ promoters, compared to the positive control. These results were in line with previous studies. This might still be within error margins, since Nsp14 had higher error bars throughout all assays. However, it is not uncommon for non-native proteins to stimulate innate immunity pathways, as shown by previous studies with SARS-CoV-2 proteins (Lei et al. 2020). The non-inhibitory activity of Nsp14 makes it a prime candidate for an internal control in any further assays with Nsp constructs, since it is in the same expression plasmid, has been produced by the same company, and has been successfully detected in WB. The last part is especially important, since it allows to confirm that the absence of detectable protein expression is not the source of the non-inhibitory effect detected in activation assays.

Although the IFA determined that SARS-CoV-2 ORF9B is not immunogenic, this result needs to be confirmed. Even though it was shown with IFA that ORF9B is expressed in Huh7 cells with IFA, it is possible that the protein is folded incorrectly, or that the HA-tag had been cleaved off, to which the primary antibodies then bound. Without WB results, it is impossible to determine if the size of the detected protein is correct. However, due to ORF9B's small size (10,8 kDa), its detection with WB is a difficult, if

not even impossible task. On the other hand, the small size, and the fact that ORF9B is an accessory protein expressed inside the host cell during infection supports the results obtained in this study, that SARS-CoV-2 ORF9B is not immunogenic.

## 6. Conclusions

The ongoing SARS-CoV-2 pandemic that started in December 2019 in Wuhan, People's Republic of China has indisputably shown that the coronavirus family is still a family from which potent human pathogens can emerge and thus should be closely monitored. The rapid spread of SARS-CoV-2 around the world beginning in December 2019 forced many countries to close their borders and limit the movement of their citizens to prevent the overloading of their health institutions, underlining the threat posed by this new coronavirus, and the importance of research on it. Despite the enormous amount of resources that have been poured into SARS-CoV-2 research, many aspects of the virus are still unknown. The long-lasting effects on the survivors of the infection and the death toll claimed by the virus show that it is critical to determine the proteins that are important to the functionality of the virus so that the development of anti-viral drugs that can target them may begin, and that infections can be diagnosed more efficiently. Equally important is the discovery of immunogenic components, so that efficient vaccines can be developed. Many vaccines have already been developed, but most of them rely on the spike-protein, which may not be the most optimal immunogenic component due to its potential for mutations to avoid neutralizing antibodies.

In this study, it was shown that at least three of the SARS-CoV-2 non-structural proteins have inhibitory effects on the RIG-I pathway, an important innate immunity signaling pathway. The information we gleaned with our methods concerned mainly the activation of IFN-λ promoter. It shows that SARS-CoV-2 Nsp1, Nsp6, and Nsp13 inhibit the activation of the IFN-λ promoter. Additionally, we showed that ORF9B is not immunogenic, contrary to what was claimed in another study (Jiang et al. 2020).

To further understand how these Nsps inhibit the RIG-I pathway, different components of the RIG-I pathway, such as MAVS or IKKε, could be used identify the protein that the Nsp is inhibiting and begin to study the mechanism of this inhibition. The mechanistic information would be invaluable on the antiviral drug-design front. To get a more realistic view of the function and role of the Nsps in the inhibition of RIG-I pathway and their other functions, infection studies could be utilized. This could provide

information about the interactions of host cell proteins and other viral proteins with the inhibiting Nsps.

All in all, SARS-CoV-2 will likely join the seasonal coronaviruses and circulate around the globe for the foreseeable future. This makes it necessary to continue research on SARS-CoV-2, not only to understand it, but to be prepared for another pathogenic coronavirus, that will surely emerge at some point in the future.

## Sources


Aderem, A. & Underhill, D.M. (1999) MECHANISMS OF PHAGOCYTOSIS IN MACROPHAGES. *Annu Rev Immunol* **17**:593-623.

Ahmad, L., Zhang, S., Casanova, J. & Sancho-Shimizu, V. (2016) Human TBK1: A Gatekeeper of Neuroinflammation. *Trends Mol Med* **22**:511-527.

Andersen, K.G., Rambaut, A., Lipkin, W.I., Holmes, E.C. & Garry, R.F. (2020) The proximal origin of SARS-CoV-2. *Nat Med* **26**:450-452.

Arya, R., Kumari, S., Pandey, B., Mistry, H., Bihani, S.C., Das, A., Prashar, V., Gupta, G.D., Panicker, L. & Kumar, M. (2021) Structural insights into SARS-CoV-2 proteins. *J Mol Biol* **433**:166725.

Astuti, I. & Ysrafil (2020) Severe Acute Respiratory Syndrome Coronavirus 2 (SARS-CoV-2): An overview of viral structure and host response. *Diabetes & metabolic syndrome clinical research & reviews; Diabetes Metab Syndr* **14**:407-412.

Bouhaddou, M., Memon, D., Meyer, B., White, K.M., Rezelj, V.V., Correa Marrero, M., Polacco, B.J., Melnyk, J.E., Ulferts, S., Kaake, R.M., Batra, J., Richards, A.L., Stevenson, E., Gordon, D.E., Rojc, A., Obernier, K., Fabius, J.M., Soucheray, M., Miorin, L., Moreno, E., Koh, C., Tran, Q.D., Hardy, A., Robinot, R., Vallet, T., Nilsson-Payant, B., Hernandez-Armenta, C., Dunham, A., Weigang, S., Knerr, J., Modak, M., Quintero, D., Zhou, Y., Dugourd, A., Valdeolivas, A., Patil, T., Li, Q., Hüttenhain, R., Cakir, M., Muralidharan, M., Kim, M., Jang, G., Tutuncuoglu, B., Hiatt, J., Guo, J.Z., Xu, J., Bouhaddou, S., Mathy, C.J.P., Gaulton, A., Manners, E.J., Félix, E., Shi, Y., Goff, M., Lim, J.K., McBride, T., O'Neal, M.,C., Cai, Y., Chang, J.C.J., Broadhurst, D.J., Klippsten, S., De wit, E., Leach, A.R., Kortemme, T., Shoichet, B., Ott, M., Saez-Rodriguez, J., tenOever, B.R., Mullins, R.D., Fischer, E.R., Kochs, G., Grosse, R., García-Sastre, A., Vignuzzi, M., Johnson, J.R., Shokat, K.M., Swaney, D.L., Beltrao, P. & Krogan, N.J. (2020) The Global Phosphorylation Landscape of SARS-CoV-2 Infection. *Cell* **182**:685-712.e19.

Bouvet, M., Lugari, A., Posthuma, C.C., Zevenhoven, J.C., Bernard, S., Betzi, S., Imbert, I., Canard, B., Guillemot, J., Lécine, P., Pfefferle, S., Drosten, C., Snijder, E.J., Decroly, E. & Morelli, X. (2014) Coronavirus Nsp10, a Critical Co-factor for Activation of Multiple Replicative Enzymes. *J Biol Chem* **289**:25783-25796.

Bulet, P., Stöcklin, R. & Menin, L. (2004) Anti-microbial peptides: from invertebrates to vertebrates. *Immunol Rev* **198**:169-184.

Cantuti-Castelvetri, L., Ojha, R., Pedro, L.D., Djannatian, M., Franz, J., Kuivanen, S., van der Meer, F., Kallio, K., Kaya, T., Anastasina, M., Smura, T., Levanov, L., Szirovicza, L., Tobi, A., Kallio-Kokko, H., Osterlund, P., Joensuu, M., Meunier, F.A., Butcher, S.J., Winkler, M.S., Mollenhauer, B., Helenius, A., Gokce, O., Teesalu, T., Hepojoki, J., Vapalahti, O., Stadelmann, C., Balistreri, G. & Simons, M. (2020) Neuropilin-1 facilitates SARS-CoV-2 cell entry and infectivity. *Science* **370**:856-860.

Chakraborty, D., Agrawal, A. & Maiti, S. (2021) Rapid identification and tracking of SARS-CoV-2 variants of concern. *Lancet* **397**:1346-1347.

Chan, J.F., Kok, K., Zhu, Z., Chu, H., To, K.K., Yuan, S. & Yuen, K. (2020) Genomic characterization of the 2019 novel human-pathogenic coronavirus isolated from a patient with atypical pneumonia after visiting Wuhan. *EMERG MICROBES INFEC* **9**:221-236.

CHAN-YEUNG, M. & XU, R. (2003) SARS: epidemiology. *Respirology* **8**:S9-S14.

Chau, T., Gioia, R., Gatot, J., Patrascu, F., Carpentier, I., Chapelle, J., O'Neill, L., Beyaert, R., Piette, J. & Chariot, A. (2008) Are the IKKs and IKK-related kinases TBK1 and IKK-ε similarly activated? *Trends Biochem Sci* **33**:171-180.

Chen, X., Yang, X., Zheng, Y., Yang, Y., Xing, Y. & Chen, Z. (2014) SARS coronavirus papain-like protease inhibits the type I interferon signaling pathway through interaction with the STING-TRAF3- TBK1 complex. *Protein Cell* **5**:369-381.

Chen, Y., Liu, Q. & Guo, D. (2020) Emerging coronaviruses: Genome structure, replication, and pathogenesis. *J Med Virol* **92**:418-423.

Claverie, J. (2020) A Putative Role of de-Mono-ADP-Ribosylation of STAT1 by the SARS-CoV-2 Nsp3 Protein in the Cytokine Storm Syndrome of COVID-19. *VIRUSES-BASEL* **12**:646.

Cornillez-Ty, C., Liao, L., Yates III, J.,R., Kuhn, P. & Buchmeier, M.J. (2009) Severe Acute Respiratory Syndrome Coronavirus Nonstructural Protein 2 Interacts with a Host Protein Complex Involved in Mitochondrial Biogenesis and Intracellular Signaling. *J Virol* **83**:10314-10318.

Cottam, E.M., Whelband, M.C. & Wileman, T. (2014) Coronavirus NSP6 restricts autophagosome expansion. *AUTOPHAGY* **10**:1426-1441.

Cui, J., Li, F. & Shi, Z. (2019) Origin and evolution of pathogenic coronaviruses. *NAT REV MICROBIOL* **17**:181-192.

Dunkelberger, J.R. & Song, W. (2010) Complement and its role in innate and adaptive immune responses. *Cell Res* **20**:34-50.

Egloff, M., Ferron, F., Campanacci, V., Longhi, S., Rancurel, C., Dutartre, H., Snijder, E.J., Gorbalenya, A.E., Cambillau, C. & Canard, B. (2004) The Severe Acute Respiratory Syndrome-Coronavirus Replicative Protein nsp9 Is a Single-Stranded RNA-Binding Subunit Unique in the RNA Virus World. *P NATL ACAD SCI USA* **101**:3792-3796.

Flores, J. (2018) Pale Rider: The Spanish Flu of 1918 and How It Changed the World, by Laura Spinney. *Proceedings - Baylor University.Medical Center* **31**:254.

Forni, D., Cagliani, R., Clerici, M. & Sironi, M. (2016) Molecular Evolution of Human Coronavirus Genomes. *Trends Microbiol* **25**:35-48.

Fouchier, R.A.M., Hartwig, N.G., Bestebroer, T.M., Niemeyer, B., De Jong, J.C., Simon, J.H. & Osterhaus, Albert D M E (2004) A Previously Undescribed Coronavirus Associated with Respiratory Disease in Humans. *Proceedings of the National Academy of Sciences - PNAS* **101**:6212-6216.

Gad, H.H., Dellgren, C., Hamming, O.J., Vends, S., Paludan, S.R. & Hartmann, R. (2009) Interferon-λ Is Functionally an Interferon but Structurally Related to the Interleukin-10 Family. *J Biol Chem* **284**:20869-20875.

Gao, Y., Yan, L., Huang, Y., Liu, F., Zhao, Y., Cao, L., Wang, T., Sun, Q., Ming, Z., Zhang, L., Ge, J., Zheng, L., Zhang, Y., Wang, H., Zhu, Y., Zhu, C., Hu, T., Hua, T., Zhang, B., Yang, X., Li, J., Yang, H., Liu, Z., Xu, W., Guddat, L.W., Wang, Q., Lou, Z. & Rao, Z. (2020) Structure of the RNA-dependent RNA polymerase from COVID-19 virus. *Science* **368**:779-782.

Gordon, D.E., Jang, G.M., Bouhaddou, M., Xu, J., White, K.M., O'Meara, M.,J., Rezelj, V.V., Swaney, D.L., Tummino, T.A., Foussard, H., Batra, J., Haas, K., Modak, M., Kim, M., Braberg, H., Fabius, J.M., Eckhardt, M., Soucheray, M., Cakir, M., McGregor, M.J., Li, Q., Vallet, T., Mac Kain, A., Miorin, L., Moreno, E., Zhou, Y., Peng, S., Shi, Y., Zhang, Z., Shen, W., Melnyk, J.E., Chorba, J.S., Lou, K., Dai, S.A., Barrio-Hernandez, I., Lyu, J., Mathy, C.J.P., Perica, T., Pilla, K.B., Ganesan, S.J., Saltzberg, D.J., Rakesh, R., Liu, X., Rosenthal, S.B., Calviello, L., Lin, Y., Huang, X., Liu, Y., Bohn, M., Safari, M., Ugur, F.S., Koh, C., Savar, N.S., Tran, Q.D., Fletcher, S.J., O'Neal, M.,C., Chang, J.C.J., Broadhurst, D.J., Klippsten, S., Sharp, P.P., Wenzell, N.A., Kuzuoglu-Ozturk, D., Wang, H., Trenker, R., Young, J.M., Cavero, D.A., Hiatt, J., Roth, T.L., Rathore, U., Subramanian, A., Noack, J., Hubert, M., Stroud, R.M., Frankel, A.D., Rosenberg, O.S., Verba, K.A., Agard, D.A., Ott, M., Emerman, M., Jura, N., von Zastrow, M., Verdin, E., Ashworth, A., Schwartz, O., d'Enfert, C., Mukherjee, S., Jacobson, M., Malik, H.S., Craik, C.S., Floor, S.N., Fraser, J.S., Gross, J.D., Roth, B.L., Ruggero, D., Taunton, J., Beltrao, P., García-Sastre, A., Shokat, K.M.,

Shoichet, B.K. & Krogan, N.J. (2020) A SARS-CoV-2 protein interaction map reveals targets for drug repurposing. *Nature* **583**:459-468.

Gurung, A.B. (2020) In silico structure modelling of SARS-CoV-2 Nsp13 helicase and Nsp14 and repurposing of FDA approved antiviral drugs as dual inhibitors. *Gene reports* **21**:100860.

Guthmiller, J.J. & Wilson, P.C. (2020) Remembering seasonal coronaviruses. *Science* **370**:1272-1273.

Hamre, D. & Procknow, J.J. (1966) A New Virus Isolated from the Human Respiratory Tract. *Proceedings of the Society for Experimental Biology and Medicine* **121**:190-193.

Harcourt, B.H., Jukneliene, D., Kanjanahaluethai, A., Bechill, J., Severson, K.M., Smith, C.M., Rota, P.A. & Baker, S.C. (2004) Identification of Severe Acute Respiratory Syndrome Coronavirus Replicase Products and Characterization of Papain-Like Protease Activity. *J Virol* **78**:13600-13612.

Hillen, H.S., Kokic, G., Farnung, L., Dienemann, C., Tegunov, D. & Cramer, P. (2020) Structure of replicating SARS-CoV-2 polymerase. *Nature* **584**:154-156.

Hoffmann, M., Kleine-Weber, H., Schroeder, S., Krüger, N., Herrler, T., Erichsen, S., Schiergens, T.S., Herrler, G., Wu, N., Nitsche, A., Müller, M.,A., Drosten, C. & Pöhlmann, S. (2020) SARS-CoV-2 Cell Entry Depends on ACE2 and TMPRSS2 and Is Blocked by a Clinically Proven Protease Inhibitor. *Cell* **181**:271-280.e8.

Huang, C., Wang, Y., Li, X., Ren, L., Zhao, J., Hu, Y., Zhang, L., Fan, G., Xu, J., Gu, X., Cheng, Z., Yu, T., Xia, J., Wei, Y., Wu, W., Xie, X., Yin, W., Li, H., Liu, M., Xiao, Y., Gao, H., Guo, L., Xie, J., Wang, G., Jiang, R., Gao, Z., Jin, Q., Wang, J. & Cao, B. (2020) Clinical features of patients infected with 2019 novel coronavirus in Wuhan, China. *Lancet* **395**:497-506.

Huston, N.C., Wan, H., Strine, M.S., de Cesaris Araujo Tavares, Rafael, Wilen, C.B. & Pyle, A.M. (2021) Comprehensive in vivo secondary structure of the SARS-CoV-2 genome reveals novel regulatory motifs and mechanisms. *Mol Cell* **81**:584-598.e5.

Isaacs, A. & Lindenmann, J. (2015) Virus interference. I. The interferon. *J Immunol* **195**:1911-1920.

Jiang, H., Li, Y., Zhang, H., Wang, W., Yang, X., Qi, H., Li, H., Men, D., Zhou, J. & Tao, S. (2020) SARS-CoV-2 proteome microarray for global profiling of COVID-19 specific IgG and IgM responses. *NAT COMMUN* **11**:3581.

Kim, D., Lee, J., Yang, J., Kim, J.W., Kim, V.N. & Chang, H. (2020) The Architecture of SARS-CoV-2 Transcriptome. *Cell* **181**:914-921.e10.

Kumar, M., Taki, K., Gahlot, R., Sharma, A. & Dhangar, K. (2020) A chronicle of SARS-CoV-2: Part-I - Epidemiology, diagnosis, prognosis, transmission and treatment. *Sci Total Environ* **734**:139278.

Lei, J., Kusov, Y. & Hilgenfeld, R. (2018) Nsp3 of coronaviruses: Structures and functions of a large multi-domain protein. *ANTIVIR RES* **149**:58-74.

Lei, X., Dong, X., Ma, R., Wang, W., Xiao, X., Tian, Z., Wang, C., Wang, Y., Li, L., Ren, L., Guo, F., Zhao, Z., Zhou, Z., Xiang, Z. & Wang, J. (2020) Activation and evasion of type I interferon responses by SARS-CoV-2. *Nat Commun* **11**.

Li, X., Sun, L., Seth, R.B., Pineda, G. & Chen, Z.J. (2005) Hepatitis C Virus Protease NS3/4A Cleaves Mitochondrial Antiviral Signaling Protein off the Mitochondria to Evade Innate Immunity. *P NATL ACAD SCI USA* **102**:17717-17722.

Littler, D.R., Gully, B.S., Colson, R.N. & Rossjohn, J. (2020) Crystal Structure of the SARS-CoV-2 Non-structural Protein 9, Nsp9. *ISCIENCE* **23**:101258.

Loo, Y. & Gale, M. (2011) Immune Signaling by RIG-I-like Receptors. *Immunity* **34**:680-692.

Lu, G., Hu, Y., Wang, Q., Qi, J., Gao, F., Li, Y., Zhang, Y., Zhang, W., Yuan, Y., Bao, J., Zhang, B., Shi, Y., Yan, J. & Gao, G.F. (2013) Molecular basis of binding between novel human coronavirus MERS-CoV and its receptor CD26. *Nature* **500**:227-231.

Ma, J., Chen, Y., Wu, W. & Chen, Z. (2021) Structure and Function of N-Terminal Zinc Finger Domain of SARS-CoV-2 NSP2. *Virol Sin*.

McIntosh, K., Dees, J.H., Becker, W.B., Kapikian, A.Z. & Chanock, R.M. (1967) Recovery in Tracheal Organ Cultures of Novel Viruses from Patients with Respiratory Disease. *Proceedings of the National Academy of Sciences - PNAS* **57**:933-940.

Moustaqil, M., Ollivier, E., Chiu, H., Van Tol, S., Rudolffi-Soto, P., Stevens, C., Bhumkar, A., Hunter, D.J.B., Freiberg, A.N., Jacques, D., Lee, B., Sierecki, E. & Gambin, Y. (2021) SARS-CoV-2 proteases PLpro and 3CLpro cleave IRF3 and critical modulators of inflammatory pathways (NLRP12 and TAB1): implications for disease presentation across species. *Emerging microbes & infections; Emerg Microbes Infect* **10**:178-195.

Naqvi, A.A.T., Fatima, K., Mohammad, T., Fatima, U., Singh, I.K., Singh, A., Atif, S.M., Hariprasad, G., Hasan, G.M. & Hassan, M.I. (2020) Insights into SARS-CoV-2 genome, structure, evolution, pathogenesis and therapies: Structural genomics approach. *BBA-MOL BASIS DIS* **1866**:165878.

Onomoto, K., Onoguchi, K. & Yoneyama, M. (2021) Regulation of RIG-I-like receptor-mediated signaling: interaction between host and viral factors. *Cellular & molecular immunology* **18**:539-555.

Oran, D.P. & Topol, E.J. (2020) Prevalence of Asymptomatic SARS-CoV-2 Infection A Narrative Review. *Ann Intern Med* **173**:362-367.

Palm, N.W. & Medzhitov, R. (2009) Pattern recognition receptors and control of adaptive immunity. *Immunol Rev* **227**:221-233.

Raj, R. (2021) Analysis of non-structural proteins, NSPs of SARS-CoV-2 as targets for computational drug designing. *Biochemistry and biophysics reports; Biochem Biophys Rep* **25**:100847.

Redondo, N., Zaldívar-López, S., Garrido, J.J. & Montoya, M. (2021) SARS-CoV-2 Accessory Proteins in Viral Pathogenesis: Knowns and Unknowns. *Frontiers in immunology* **12**:708264.

Sadler, A.J. & Williams, B.R.G. (2008) Interferon-inducible antiviral effectors. *NAT REV IMMUNOL* **8**:559-568.

Samuel, C.E. (2001) Antiviral Actions of Interferons. *Clin Microbiol Rev* **14**:778-809.

Sarkar, M. & Saha, S. (2020) Structural insight into the role of novel SARS-CoV-2 E protein: A potential target for vaccine development and other therapeutic strategies. *PLOS ONE* **15**:e0237300.

Schiavina, M., Pontoriero, L., Uversky, V.N., Felli, I.C. & Pierattelli, R. (2021) The highly flexible disordered regions of the SARS-CoV-2 nucleocapsid N protein within the 1–248 residue construct: sequence-specific resonance assignments through NMR. *Biomolecular NMR assignments; Biomol NMR Assign* **15**:219-227.

Schlee, M. (2013) Master sensors of pathogenic RNA – RIG-I like receptors. *Immunobiology* **218**:1322-1335.

Schroder, K., Hertzog, P.J., Ravasi, T. & Hume, D.A. (2004) Interferon-γ: an overview of signals, mechanisms and functions. *J LEUKOCYTE BIOL* **75**:163-189.

Schubert, K., Karousis, E.D., Jomaa, A., Scaiola, A., Echeverria, B., Gurzeler, L., Leibundgut, M., Thiel, V., Mühlemann, O. & Ban, N. (2020) SARS-CoV-2 Nsp1 binds the ribosomal mRNA channel to inhibit translation. *NAT STRUCT MOL BIOL* **27**:959-966.

Scott, I. (2010) The role of mitochondria in the mammalian antiviral defense system. *MITOCHONDRION* **10**:316-320.

Seaman, M.N.J., Gautreau, A. & Billadeau, D.D. (2013) Retromer-mediated endosomal protein sorting: all WASHed up. *Trends Cell Biol* **23**:522-528.

Shors, T. (2017) Understanding Viruses, Jones & Bartlett Learning, Burlington, Massachusetts.

Su, S., Wong, G., Shi, W., Liu, J., Lai, A.C.K., Zhou, J., Liu, W., Bi, Y. & Gao, G.F. (2016) Epidemiology, Genetic Recombination, and Pathogenesis of Coronaviruses. *Trends Microbiol* **24**:490-502.

Sun, J.C., Lopez-Verges, S., Kim, C.C., DeRisi, J.L. & Lanier, L.L. (2011) NK cells and immune "memory". *J Immunol* **186**:1891-1897.

Suryawanshi, R.K., Koganti, R., Agelidis, A., Patil, C.D. & Shukla, D. (2021) Dysregulation of Cell Signaling by SARS-CoV-2. *Trends Microbiol* **29**:224-237.

Tabibzadeh, A., Esghaei, M., Soltani, S., Yousefi, P., Taherizadeh, M., Safarnezhad Tameshkel, F., Golahdooz, M., Panahi, M., Ajdarkosh, H., Zamani, F. & Karbalaie Niya, M.H. (2021) Evolutionary study of COVID-19, severe acute respiratory syndrome coronavirus 2 (SARS-CoV-2) as an emerging coronavirus: Phylogenetic analysis and literature review. *Veterinary medicine and science; Vet Med Sci* **7**:559-571.

Tanner, J.A., Watt, R.M., Chai, Y., Lu, L., Lin, M.C., Peiris, J.S.M., Poon, L.L.M., Kung, H. & Huang, J. (2003) The Severe Acute Respiratory Syndrome (SARS) Coronavirus NTPase/Helicase Belongs to a Distinct Class of 5′ to 3′ Viral Helicases. *J Biol Chem* **278**:39578-39582.

Te Velthuis, Aartjan J. W, Van Den Worm, Sjoerd H.,E. & Snijder, E.J. (2012) The SARS-coronavirus nsp7+nsp8 complex is a unique multimeric RNA polymerase capable of both de novo initiation and primer extension. *Nucleic Acids Res* **40**:1737-1747.

Thomas, S. (2020) The structure of the membrane protein of sars-cov-2 resembles the sugar transporter semisweet. *Pathogens & immunity* **5**:342-363.

Tu, Y., Chien, C., Yarmishyn, A.A., Lin, Y., Luo, Y., Lin, Y., Lai, W., Yang, D., Chou, S., Yang, Y., Wang, M. & Chiou, S. (2020) A Review of SARS-CoV-2 and the Ongoing Clinical Trials. *INT J MOL SCI* **21**:2657.

Unterholzner, L. & Bowie, A.G. (2008) Viral evasion and subversion of pattern-recognition receptor signalling. *Nature reviews. Immunology* **8**:911-922.

V'kovski, P., Kratzel, A., Steiner, S., Stalder, H. & Thiel, V. (2020) Coronavirus biology and replication: implications for SARS-CoV-2. *Nature reviews.Microbiology; Nat Rev Microbiol* **19**:155-170.

Vabret, A., Mourez, T., Dina, J., van der Hoek, L., Gouarin, S., Petitjean, J., Brouard, J. & Freymuth, F. (2005) Human coronavirus NL63, France. *EMERG INFECT DIS* **11**:1225-1229.

Wack, A., Terczyńska-Dyla, E. & Hartmann, R. (2015) Guarding the frontiers: The biology of type III interferons. *Nat Immunol* **16**:802-809.

Walls, A.C., Park, Y., Tortorici, M.A., Wall, A., McGuire, A.T. & Veesler, D. (2020) Structure, Function, and Antigenicity of the SARS-CoV-2 Spike Glycoprotein. *Cell* **183**:1735.

Wang, S., Trilling, M., Sutter, K., Dittmer, U., Lu, M., Zheng, X., Yang, D. & Liu, J. (2020) A Crowned Killer's Resume: Genome, Structure, Receptors, and Origin of SARS-CoV-2. *Virol Sin* **35**:673-684.

Wang, Y., Landeras-Bueno, S., Hsieh, L., Terada, Y., Kim, K., Ley, K., Shresta, S., Saphire, E.O. & Regla-Nava, J. (2020) Spiking Pandemic Potential: Structural and Immunological Aspects of SARS-CoV-2. *Trends Microbiol* **28**:605-618.

WEISS, S.R. & NAVAS-MARTIN, S. (2005) Coronavirus Pathogenesis and the Emerging Pathogen Severe Acute Respiratory Syndrome Coronavirus. *Microbiology and Molecular Biology Reviews* **69**:635-664.

Woo, P.C.Y., Lau, S.K.P., Chu, C., Chan, K., Tsoi, H., Huang, Y., Wong, B.H.L., Poon, R.W.S., Cai, J.J., Luk, W., Poon, L.L.M., Wong, S.S.Y., Guan, Y., Peiris, J.S.M. & Yuen, K. (2005) Characterization and Complete Genome Sequence of a Novel Coronavirus, Coronavirus HKU1, from Patients with Pneumonia. *J Virol* **79**:884-895.

Wrapp, D., Wang, N., Corbett, K.S., Goldsmith, J.A., Hsieh, C., Abiona, O., Graham, B.S. & McLellan, J.S. (2020) Cryo-EM structure of the 2019-nCoV spike in the prefusion conformation. *Science* **367**:1260.

Wu, B. & Hur, S. (2015) How RIG-I like receptors activate MAVS. *CURR OPIN VIROL* **12**:91-98.

Xia, H., Cao, Z., Xie, X., Zhang, X., Chen, J.Y., Wang, H., Menachery, V.D., Rajsbaum, R. & Shi, P. (2020) Evasion of Type I Interferon by SARS-CoV-2. *CELL REP* **33**:108234.

Ye, Q., West, A.M.V., Silletti, S. & Corbett, K.D. (2020) Architecture and self-assembly of the SARS-CoV-2 nucleocapsid protein. *Protein Sci* **29**:1890-1901.

Zaki, A.M., van Boheemen, S., Bestebroer, T.M., Osterhaus, Albert D. M. E. & Fouchier, R.A.M. (2012) Isolation of a Novel Coronavirus from a Man with Pneumonia in Saudi Arabia. *NEW ENGL J MED* **367**:1814-1820.

Zdrenghea, M.T., Makrinioti, H., Muresan, A., Johnston, S.L. & Stanciu, L.A. (2015) The role of macrophage IL-10/innate IFN interplay during virus-induced asthma. *Rev Med Virol* **25**:33-49.

Zhu, N., Zhang, D., Wang, D., Wang, W., Li, X., Yang, B., Song, J., Zhao, X., Huang, B., Shi, W., Lu, R., Niu, P., Zhan, F., Ma, X., Xu, W., Wu, G., Gao, G.F. & Tan, W. (2020) A Novel Coronavirus from Patients with Pneumonia in China, 2019. *NEW ENGL J MED* **382**:727-733.